Mon. Not. R. Astron. Soc. **000**, Vol. 291–3, p. 527–543 (1997) Printed 12 September 1997 (MN LaTeX style file v1.4)

The $\mathbf{Mg}_b$–σ Relation of Elliptical Galaxies at $z \approx 0.37$ ⋆

Bodo L. Ziegler†‡ and Ralf Bender

Institut für Astronomie und Astrophysik der Ludwigs–Maximilian–Universität, Universitätssternwarte, Scheinerstraße 1, 81679 München, Germany

Accepted June 23 1997 . Received 1997 June 23; in original form 1997 February 14

ABSTRACT

We derive absorption line indices of elliptical galaxies in clusters at intermediate redshift ($z \approx 0.37$) from medium-resolution spectroscopy together with kinematical parameters. These galaxies exhibit a relationship between the linestrength of Mg_b ($\lambda_0 \approx 5170$ Å) and their internal velocity dispersion σ similar to local dynamically hot galaxies. But for any given σ, the Mg_b linestrength of the distant ellipticals is significantly lower than the mean value of the nearby sample. The difference of Mg_b between the two samples is small ($\langle\Delta\mathrm{Mg}_b\rangle \approx -0.4$ Å) and can be fully attributed to the younger age of the distant stellar populations in accordance with the passive evolution model for elliptical galaxies. The low reduction of Mg_b at a look–back time of about 5 Gyr requires that the bulk of the stars in cluster ellipticals have formed at very high redshifts of $z_f > 2$. For the most massive galaxies, where the reduction is even lower, z_f probably exceeds 4.

Unlike most methods to measure the evolution of elliptical galaxies using luminosities, surface brightnesses or colours, the Mg_b–σ test does not depend on corrections for extinction and cosmic expansion (K–correction) and only very little on the slope of the initial mass function. The combination of a kinematical parameter with a stellar population indicator allows us to study the evolution of very similar objects. In addition, the good mass estimate provided by σ means that the selection criteria for the galaxy sample as a whole are well controlled.

In quantitative agreement with the reduction of the Mg_b absorption we find an increase of the B magnitude of $\langle\Delta\mathrm{M}_B\rangle \approx -0.5$ mag at fixed σ from the Faber–Jackson relation. The brightening of the ellipticals at $z = 0.37$ arises solely from the evolution of their stellar populations and is of the same order as the change in magnitudes when varying the deceleration parameter q_0 from -0.5 to $+0.5$ at this redshift.

Studying the evolution of the Mg_b–σ relation in combination with that of the Faber–Jackson relation allows us to constrain both the slope of the initial mass function and the value of the deceleration parameter. Our current data (including measurement errors) are compatible with the standard Salpeter IMF and $q_0 = 0.5 \pm 0.5$.

Key words: galaxies: elliptical and lenticular, cD – galaxies: evolution – galaxies: formation – galaxies: stellar content

1 INTRODUCTION

Twenty years after the seminal papers on the formation of elliptical galaxies by Larson (1975) and by Toomre (1977) there is still much disagreement among the astronomical community on both the process of formation and the evolution of early-type galaxies. Is an elliptical galaxy formed in a single collapse or via merging? Was there a short epoch of formation or have ellipticals been formed continuously by hierchical merging at similar levels? What is the influence of the density environment? Once created, is the stellar population of ellipticals evolving just passively or do minor merging/accretion events drastically change their characteristics frequently?

In the local universe, ongoing merging is observed and it is generally assumed that most of the 'ultraluminous' *IRAS*

⋆ Partly based on observations carried out at the European Southern Observatory, La Silla, Chile.

† Visiting astronomer of the German–Spanish Astronomical Center, Calar Alto, operated by the Max–Planck–Institut für Astronomie, Heidelberg, jointly with the Spanish National Commission for Astronomy.

‡ E-mail: ziegler@usm.uni-muenchen.de

galaxies represent merging processes (Schweizer 1990). Numerical simulations show in great detail how the merging of two spiral galaxies leads to the formation of a stellar system with a de Vaucouleurs profile (Barnes & Hernquist 1992). Often, a core kinematically decoupled from the main body is found in the interior of such simulated merger products, implying that most of the ellipticals observed to have a decoupled core were formed in a merger. More generally, elliptical galaxies with boxy or irregular isophotes are thought to be the result of mergers/interactions (Bender et al. 1989) indicating that at least two-thirds of all bright ellipticals have a merger origin.

Morphological and spectroscopic examinations of galaxy clusters at intermediate redshifts have shown that the 'Butcher–Oemler effect' is the result, not of a significantly increasing merger rate, but of the increasing star formation activity of disk galaxies with redshift (e.g. Dressler et al. 1994). Rather, the very low scatter in the optical/infrared colour–magnitude diagrams (Bower, Lucey, & Ellis 1992) and the Mg_2–σ relation (Bender, Burstein, & Faber 1993) of massive elliptical galaxies in nearby clusters is compatible with a short formation epoch at a high redshift ($z_f > 2$), implying that recent mergers add only a very small fraction to the total number of cluster ellipticals. Indeed, stellar population synthesis models can fit best the spectral energy distribution of observed local ellipticals assuming a short period of star formation followed by 'passive' evolution of the stellar population without any significant new star formation at later times (e.g. Bruzual & Charlot 1993). Recently, accurate measurements of physical relations of early-type galaxies at intermediate redshifts ($z \approx 0.4$) support this passive evolution scenario. Thus, the Tolman test does not indicate a significant deviation of the surface brightness evolution from the pure cosmological dependence (e.g. Pahre, Djorgovski, & de Carvalho 1996, Schade, Barrientos, & Lopéz–Cruz 1997). Analysis of the fundamental plane yield a moderate decrease in the M/L ratio (e.g. van Dokkum & Franx 1996, Kelson et al. 1997). We presented preliminary results from an investigation of the Mg_b–σ relation showing mild evolution of the Mg_b index and the blue luminosity (Bender, Ziegler, & Bruzual 1996). In addition, observational data out to $z \approx 1$ are accumulating that are compatible with this 'passive evolution' scenario for ellipticals (or rather, the more luminous, red galaxies at higher redshifts) both in the field and in clusters. The various methods for testing evolution comprise luminosity functions and number counts (e.g. Glazebrook et al. 1995, Lilly et al. 1995, Ellis et al. 1996), optical and near infrared colour–magnitude diagrams (e.g. Aragón–Salamanca et al. 1993, Stanford, Eisenhardt, & Dickinson 1995) and projections of the fundamental plane relations (e.g. Schade et al. 1996). Taking advantage of the capability of the *Hubble* space telescope and 10m-telescopes, the search for galaxies at high redshift has just begun using both morphological and spectroscopic information. Steidel et al. (1996), for example, have found candidate precursors of ellipticals at $3 < z < 3.5$.

Semi-analytic models of galaxy formation based on cold dark matter (CDM)-like structure formation theory have shown that elliptical galaxies could have been formed in mergers and nevertheless appear so homogeneous in their stellar population as is observed in the local Universe (Kauffmann 1996). In these models, most of the stars in ellipticals formed at high redshifts ($z_f > 1.9$).
However, is the 'passive evolution' scenario valid for the whole population of nearby early–type galaxies, or could it be that the methods stated above pick up only those galaxies that comply with the assumptions of passive evolution? Using the V/V_{max}–test (Schmidt 1968), Kauffmann, Charlot, & White (1997) find that the fraction of early-type galaxies dropping out of their sample increases with redshift so that at $z \approx 1$ only about one third of the bright E and S0 galaxies seen today were already assembled. Since this investigation is based on fields of the Canada–France redshift survey that contains mostly field galaxies, their result may indicate more rapid number density evolution in the low density environment. CDM simulations by Baugh, Cole, & Frenk (1996) predict that a galaxy may change its appearance (as disk-like or spheroidal) several times during its existence. Infrared observations of M32 (Elston & Silva 1992, Freedman 1992) and the bulge of M31 (Rich & Mould 1991) resolve a population of very bright red giant stars that indicate a generation of stars only about 5 Gyr old.
In this paper, we present a new method to examine the evolution of the stellar population of elliptical galaxies with redshift based on the tight relationship between the Mg_b index and the velocity dispersion σ of elliptical galaxies. This method permits good control of the sample selection and has several advantages with respect to those mentioned above. It will be described in Section 2, wheras Section 3, 4 and 5 will deal with the sample selection, the observations and the data reduction, respectively. Our results and conclusions will be presented in Sections 6 and 7.

2 THE Mg_b–σ TEST

All dynamically hot stellar systems show the same mean relationship between central Mg_2 absorption and central velocity dispersion (σ_0) (e.g. Dressler et al. 1987, Bender, Burstein, & Faber 1993). Although these systems comprise four orders of magnitudes in mass and luminosity (ranging from the bulges of S0– and spiral galaxies up to the giant ellipticals) and their Mg_2 equivalent widths differ by up to 0.35 mag, the scatter about the mean Mg_2–σ relation is very low. The Mg_2 index as defined by the Lick system of absorption indices (Faber et al. 1985) measures the absorption of the MgH molecular band and the Mg I triplet around $\lambda_0 \approx 5173$ Å, whereas the Mg_b index measures only this triplet with respect to an adjacent pseudo-continuum. For reasons described below, the Mg_2 index can not be determined with the same accuracy as Mg_b in our target galaxies at redshifts of $z \approx 0.37$. In order to compare the Mg absorption of the distant ellipticals to published Mg_2 measurements of local ellipticals the Mg_2 values have to be converted to Mg_b. For the synthetic Mg_b and Mg_2 values calculated by Worthey (1994) for simple stellar populations (SSP) with ages between 1.5 and 17 Gyr, we find the following linear transformation (see Fig. 1):

$$\mathrm{Mg}_b\,\text{Å}^{-1} = (14.3 \ldots 15.5) \times \mathrm{Mg}_2\,\mathrm{mag}^{-1}, \qquad (1)$$

with the smaller conversion factor for a metallicity of $\lg Z/Z_\odot = +0.5$, the greater one for $\lg Z/Z_\odot = -0.5$. We

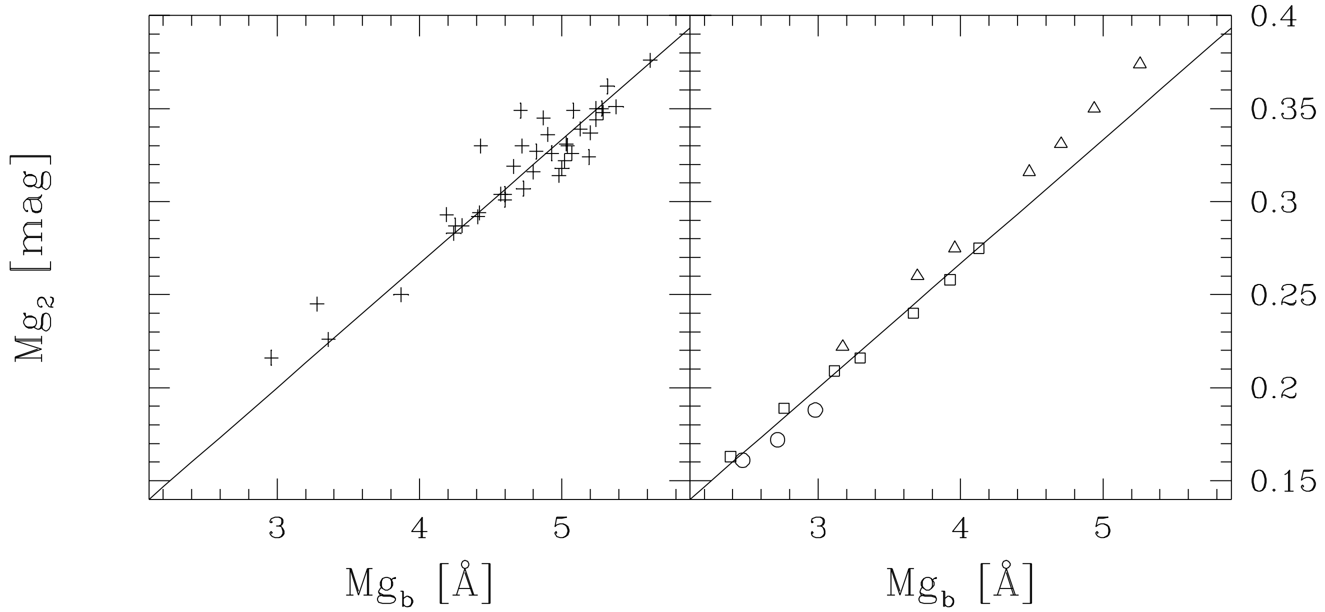

Figure 1. Mg_2 vs. Mg_b: left panel: observed data (González 1993), right panel: calculated values (Worthey 1994) for different ages (1.5, 2, 3, 6, 8, 12, and 17 Gyr) and metallicities (∘: $\lg Z/Z_\odot = -0.5$, ▫: $\lg Z/Z_\odot = 0$, ▵: $\lg Z/Z_\odot = 0.5$). The straight line corresponds to $Mg_2 = Mg_b/15$.

adopted a slope of 15, a value consistent with the observational data of a small sample of nearby ellipticals (González 1993) and in agreement with the result by Burstein et al. (1984).

Throughout this paper, we will use some 60 elliptical galaxies in the Coma and Virgo clusters as a comparison sample. A principal components analysis of the 7 Samurai data (Dressler et al. 1987) of these ellipticals yields, as best fit to the Mg_b–σ relation,

$$Mg_b\,\text{Å}^{-1} = 2.7\lg[\sigma_0/(\text{km s}^{-1})] - 1.65. \quad (2)$$

The brighter ellipticals ($\lg\sigma_0 \geq 2.3$) show a very low intrinsic scatter,

$$\sigma_{\rm intr}(Mg_b) = 0.16\,\text{Å}. \quad (3)$$

The strength of the Mg_b absorption for a single stellar population is driven mainly by metallicity and age. A bivariate polynomial fit to Worthey's SSP values yields the following dependence for metallicities $-2 < \lg Z/Z_\odot < +0.25$ and ages $t > 3$ Gyr, see Fig. 2:

$$\lg Mg_b = 0.20\lg t + 0.31\lg Z/Z_\odot + 0.37 \quad (4)$$

For solar metallicity and ages $t > 12$ Gyr, $\partial\lg Mg_b/\partial\lg t$ might be as low as 0.15. The same slopes are derived for the Bruzual & Charlot (1997) models showing that the proportionality factors in equation (4) are robust and do not depend on the population synthesis models (see also Bruzual 1996). Only the zero-point is more uncertain but this causes no problem at all because only relative changes will be considered in the following.

The tight correlation between Mg_b and velocity dispersion σ_0 of local ellipticals constrains both the relative scatter in mean age ($\Delta t/t$) and the relative scatter in mean metallicity ($\Delta Z/Z$). For the brighter ellipticals in the Coma cluster, e.g., equations 2, 3 and 4 yield

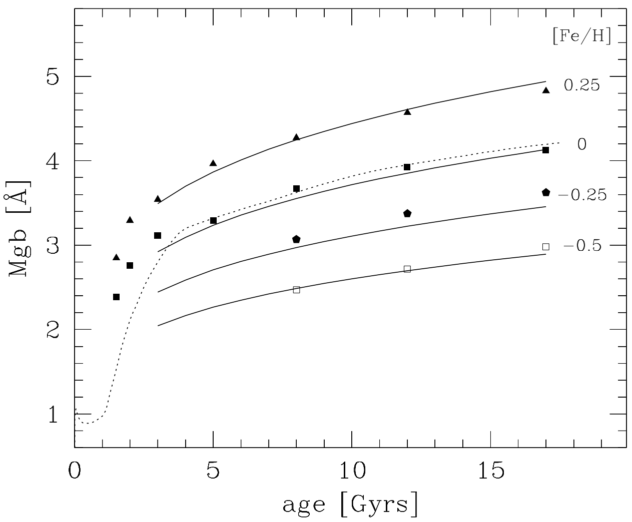

Figure 2. Dependence of the Mg_b index on metallicity and age: symbols represent values given by Worthey (1994), the dashed line corresponds to the Bruzual&Charlot (1997) model for solar metallicity, solid lines follow equation (4).

$$\Delta t/t < 0.17 \quad \text{and} \quad \Delta Z/Z < 0.11. \quad (5)$$

This narrow constraint on the age spread of cluster ellipticals implies that they did not form continuously at the same rate but that there was a rather short formation epoch of these galaxies. If, e.g., the majority of ellipticals were formed 12 Gyr ago, then the scatter in age would be about 2 Gyr.

Measuring absorption line strengths or colours alone in distant galaxies would not allow to unambiguously determine their ages because stellar population models have shown that effects of age and metallicity can compensate each other (the so-called age–metallicity degeneracy, see e.g. Worthey 1994. However, by comparing the Mg_b–σ relations at different redshifts relative mean ages of cluster ellipticals can be obtained, a method we dubbed the Mg_b–σ test (Bender, Ziegler, & Bruzual 1996). This is because the maximum scatter in $\Delta Z/Z$ for a given σ_0 is constrained to less than 11 per cent (equation (5)). If most of the elliptical galaxies evolve only passively between intermediate redshifts and today, i.e. if no dissipative major merger occured during the last few Gyr that could have disturbed the velocity dispersion or the Mg_b absorption (via a burst of star formation), then any reduction of the Mg_b linestrength of an intermediate redshift elliptical compared to the mean value of the local sample at the same velocity dispersion is the result only of the lower age of the elliptical.

Unlike those methods that use luminosity or surface brightness to determine the evolution of ellipticals, the Mg_b–σ test is independent of any k–corrections and corrections for extinction, both of which can be a source of systematic errors. In addition, the influence of the initial mass function on the amount of evolution derived from the Mg_b–σ test is negligible, because Mg_b is determined mainly by the temperature of the turn-off stars and not by the total number of giant stars. A further advantage of the Mg_b–σ test is the ability to control the selection of the different galaxy samples. Knowing the velocity dispersion of an elliptical galaxy it is possible to estimate its mass and, therefore, to study whether there is any significant difference in the mass distributions of the samples. Such a difference would distort the results, because a sample with a higher number of very massive galaxies, e.g., would also have a higher mean metallicity.

3 SAMPLE SELECTION

The 'passive evolution' model of stellar population synthesis predicts that observable characteristics of ellipticals like luminosity, colour and line indices change slower and slower with time after about 3 Gyr. Therefore, significant differences in these parameters compared to today's ellipticals are expected only at intermediate redshifts ($z > 0.3$). But, at $z = 0.3$ (for example) the Mg_b triplet is redshifted to $\lambda = 6725$ Å and falls already into that wavelength range where any spectrum is dominated by numerous and strong tellurial emission lines. In that range, the continuum of a typical giant elliptical is on average ten times lower than the mean flux level of the night sky, see upper panel of Fig. 4. The situation is even worsened by the existence of many variable absorption bands of water vapour. Thus, the maximum signal–to–noise ratio of the Mg_b absorption line can be achieved only for small redshift bins in which the influence of the Earth's atmosphere is at its minimum. The first of such ideal redshift bins is given for $0.358 < z < 0.380$, if the H_β, Mg_b, Fe 5270 and Fe 5335 indices are to be determined. At these redshifts, spectroscopically classified galaxy members have been published only for two clusters, *Abell 370* (Mellier et al. 1988, Pickles & van der Kruit 1991) and *CL 0949+44* (Dressler & Gunn 1992). To increase the number of elliptical galaxies suitable for our investigation, we carried out a photometric campaign of a sample of 20 clusters with estimated redshifts of $z \approx 0.37$ in the V, R_c and I_c bands. This study will be published in detail in another paper (see also (Ziegler 1996)). Cluster galaxies were then classified according to their $(V-R)$ and $(V-I)$ colours. Compared to the spectroscopic classification of galaxies in *Abell 370* and *CL 0949+44* the success rate for identifying E/S0 galaxies correctly was about 85 per cent. In this paper, spectroscopic data will be presented of the three clusters *Abell 370* ($z = 0.375$), *CL 0949+44* ($z = 0.377$) and *MS 1512+36* ($z = 0.372$). Out of each cluster the brightest ellipticals and a number of less luminous ones were selected for spectroscopic observation.

4 OBSERVATIONS

Spectroscopic observations were done during several campaigns using the 3.5m telescope on Calar Alto and the 3.6m telescope at the European Southern Observatory (ESO).

During five runs on Calar Alto, a Boller & Chivens twin spectrograph was used at the Cassegrain focus. The grating T04 (600 lines mm^{-1}, dispersion: 72 Å mm^{-1}) of the red channel yielded equal efficiency at all observed wavelengths. The spatial resolution of the CCD was 0.9 arcsec pixel^{-1}. Using a longslit, at least two galaxies could be observed at the same time, leaving enough space for the sky, which is essential for an accurate sky subtraction. The redshifted ellipticals were observed in the wavelength range $\lambda\lambda = 6400 - 8000$ Å with a slit width of 3.6 arcsec, chosen to collect as much light as possible and to minimize positioning problems. Comparison stars were observed at the corresponding rest frame wavelengths $\lambda\lambda = 4500 - 6100$ Å with a slit width of 2.4 arcsec, so that the spectra of both the galaxies and the stars had the same instrumental broadening of approximately 100 km s^{-1}. This arrangement is well suited for the determination of velocity dispersions of elliptical galaxies having $\sigma \approx 200 - 300$ km s^{-1}.

During two nights at the ESO 3.6m telescope, multi-object spectroscopy was achieved with the EFOSC1 focal reducer using the grism with the lowest available dispersion (RED 150, 120 Å mm^{-1}). The spectra had a lower signal–to–noise ratio than those obtained at Calar Alto, mainly because the slitlets, produced by punching round holes in a row into the multi-object mask, had a stamp-like boundary structure which severely affected the sky subtraction. Together with the rather high instrumental broadening of ~ 190 km s^{-1} (using the smallest available punch head) this resulted in the data being useful only for a comparison check with the Calar Alto data.

Because the observed galaxies have rather low apparent magnitudes (18 mag $<$ R$_c$ $<$ 20 mag), a total exposure time between 8 and 12 h was necessary to achieve at least a signal–to–noise ratio (S/N)$>$ 40 Å^{-1} at the Calar Alto 3.5m telescope. These long integration times were realized by adding up several frames with exposures of (1-1.5) h. In addition, a few white dwarfs and some red giant stars (Faber et al. 1985) were observed for the purpose of flux calibration, water vapour correction, kinematical analysis and calibration of absorption line strengths to the Lick system.

5 DATA

5.1 Photometry

For the present study the photometry had the task to yield information about the relative exact positions, the extent and the energy distribution of objects in the cluster field. For about 30 objects of each cluster the light profile was fitted by a Gaussian to derive the centre positions and the full width at half maximum (FWHM) values which enable us to discriminate between stellar and extended objects. Intensities were measured within two concentric circles around each object. The inner circle comprised most of the object flux whereas the outer ring consisted mainly of sky flux. In this way, sky subtraction was achieved accurately. The observed standard stars allowed exact flux calibration via airmass correction and colour transformation, whereas extinction correction was applied according to Burstein & Heiles (1984). The overall error of the magnitudes was estimated to be of order 0.1 mag.
The combined data allowed the selection of candidate elliptical galaxies for the follow-up spectroscopy according to their $(V-R)$ and $(V-I)$ colours. The data and contour plots of *Abell 370*, *CL 0949+44* and *MS 1512+36* are given in Appendix A.

5.1.1 *Absolute magnitudes*

In addition to the Mg_b–σ test, the evolution of elliptical galaxies can also be studied using the correlation between their luminosity and velocity dispersion (Faber & Jackson 1976). To establish the Faber–Jackson relation of the ellipticals at $z = 0.37$, their *absolute* restframe magnitudes $(B\,V\,R)_{\mathrm{rest}}$ must be determined from their observed *apparent* ones $(V\,R\,I)_{\mathrm{obs}}$. This is achieved by transforming first the *aperture* magnitudes into *total* ones from which the distance modulus (dm) and the k–correction (k_{cor}) are then subtracted,

$$M_i = m_{i,\mathrm{tot}} - dm - k_{i,\mathrm{cor}}, \qquad i = B, V, R, I. \tag{6}$$

The ratio of aperture radius (r_a) to the effective radius of the galaxy (r_e) is the important factor when extrapolating aperture magnitudes to total ones $(r_a = \infty)$. Because the r_e of the faint distant galaxies can not be measured with seeing-limited ground-based photometry we estimated these values according to the correlation between r_e and σ which can be deduced from the *fundamental plane* (FP) relations,

$$\lg(r_e/\mathrm{kpc}) = 3.4\,\lg[\sigma/(\mathrm{km\,s^{-1}})] - 6.990. \tag{7}$$

This relation is a rather good approximation for ellipticals having $\sigma > 150$ km s^{-1}, see Fig. 3. The application of the FP relations to the distant ellipticals is justified by the recent confirmation of a FP at intermediate redshifts ($z \approx 0.4$, van Dokkum & Franx 1996). To transform the r_e to apparent diameters a specific cosmology has to be chosen. For a $\Lambda = 0$ Universe, the apparent r_e in arcseconds is given by (Mattig 1958)

$$\frac{r_{e,\mathrm{as}}}{\mathrm{arcsec}} = \frac{1}{3600}\,\frac{\pi}{180}\,\frac{r_e}{\mathrm{Mpc}}\,\frac{H_0\,{q_0}^2(1+z)^2/c}{q_0 z + (q_0 - 1)(\sqrt{1+2q_0 z} - 1)}. \tag{8}$$

The aperture correction (a_{cor}) can be calculated with a growth curve (f) based on the $r^{1/4}$ law (de Vaucouleurs

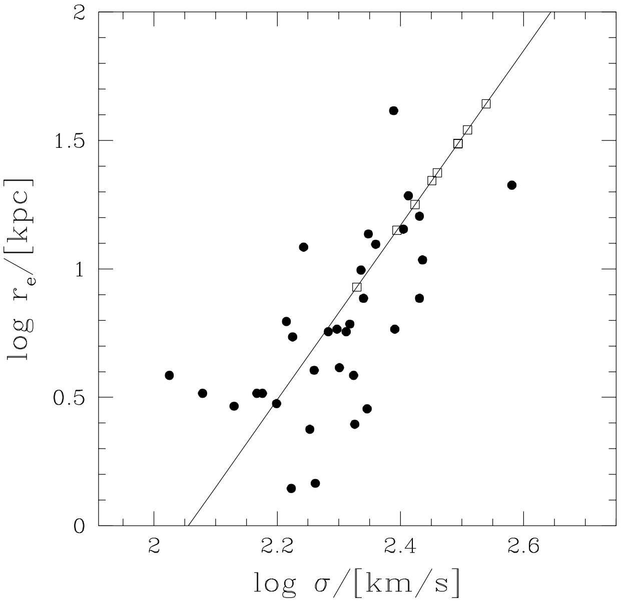

Figure 3. Correlation between effective radius r_e and velocity dispersion σ of elliptical galaxies (• measured values of Coma ellipticals, ▫ calculated values for *Abell 370* according to equation (7) (straight line) as derived from the FP relations).

1962) of the mean projected light profile of elliptical galaxies:

$$a_{\mathrm{cor}}(x(z, q_0, H_0))/\,\mathrm{mag} = -2.5\,\mathrm{lg\,f(x)} \tag{9}$$

where $x = \frac{r_a}{r_{e,\mathrm{as}}}$, $y = 7.668\,x^{1/4}$, $f = 1 - b\,e^{-y}$ and $b = 1 + \sum_{n=1}^{7} \frac{y^n}{n!}$. The influence of H_0 and q_0 on a_{cor} is increasing with r_e. For $H_0 = 50$ km s^{-1} Mpc^{-1} and $q_0 = 0.5$ the aperture corrections for the observed galaxies lie between 0.2 mag ($r_e = 10$ kpc) and 1.1 mag ($r_e = 40$ kpc). A typical error in a_{cor} of 0.2 mag was estimated from the scatter of the local r_e–σ relation by changing r_e by a factor of 3. Therefore, the uncertainty in the estimate of the effective radii determines the accurateness of the aperture corrections. The values of the total (apparent) magnitudes ($m_{\mathrm{tot}} = m_{\mathrm{obs}} - a_{\mathrm{cor}}$) change little with respect to this uncertainty when the aperture size (r_a), within which the intensities are measured, is varied. For this reason, the error in the determination of the sky background due to a wrong choice of apertures is smaller than the error introduced by the estimate of r_e.
The next step in the determination of absolute magnitudes is the calculation of the luminosity distance (d_L) of the galaxies at $z = 0.37$. This is done similarly to equation (8),

$$\frac{d_L}{\mathrm{Mpc}} = \frac{c}{H_0\,{q_0}^2}\left[q_0 z + (q_0 - 1)(\sqrt{1+2q_0 z} - 1)\right]. \tag{10}$$

Then, the distance modulus is just

$$dm/\,\mathrm{mag} = 5\,\mathrm{lg[d_L(z, q_0, H_0)]} + 25. \tag{11}$$

To determine the k–correction we have created model spectra using population synthesis (Bruzual & Charlot 1997) that matched luminosities and colours of the observed ellipticals of *Abell 370*. Model galaxies contained a stellar population which was formed within a 1-Gyr burst and evolved only passively thereafter. The model spectra allowed the measurement of both apparent 'observed' magnitudes and absolute restframe magnitudes yielding the k–corrections according to equation (6). For a redshift of $z = 0.37$ we found the following average values with uncertainties of 0.05 mag:

$$k_{\rm cor}(B_{\rm obs}, B_{\rm rest}) = 1.78\,{\rm mag}, \quad (12)$$
$$k_{\rm cor}(V_{\rm obs}, B_{\rm rest}) = 0.22\,{\rm mag}, \quad (13)$$
$$k_{\rm cor}(V_{\rm obs}, V_{\rm rest}) = 1.15\,{\rm mag}, \quad (14)$$
$$k_{\rm cor}(R_{\rm obs}, R_{\rm rest}) = 0.58\,{\rm mag}. \quad (15)$$

To study the influence of the initial mass function (IMF) on the evolution of the absolute magnitudes we created model galaxies having different x–values of the standard Salpeter parametrization $[\Phi(m) \propto m^{-(x+1)}]$. For the B magnitude, e.g., we found the following dependence, which is a good approximation for ages $t > 1.5$ Gyr:

$$\Delta B/\,{\rm mag} \approx 3.35\,\Delta\,{\rm lg(t/yr)}\,\times\,[1 - 0.24\,({\rm x} - 1.35)] \quad (16)$$

This formula is in good agreement with the one given by Tinsley (1980). For a flat Universe ($\Omega = 1$) the time dependence can be transformed into a function of redshift, because the scale factor ($R = 1/(1+z)$) then depends on time as $R \propto t^{2/3}$:

$$\Delta B/\,{\rm mag} \approx 2.18\,{\rm ln(1+z)}\,\times\,[1 - 0.24\,({\rm x} - 1.35)] \quad (17)$$

According to this formula a deviation of 1 from the Salpeter value of x (1.35) results in a change of 0.16 mag in B at the redshift of the observed galaxies ($z = 0.37$).

5.2 Spectroscopy

All spectra were carefully reduced using standard techniques (see, e.g., Bender, Saglia, & Gerhard 1994): bias and dark subtraction, flatfield division, cosmics removal, sky subtraction, logarithmic wavelength calibration, extraction of a one-dimensional spectrum and, finally, summation of the individual spectra per galaxy.

Because the galaxy spectra are heavily dominated by sky emission lines at the observed wavelengths (see Fig. 4), the following procedure was applied for the sky subtraction: In two windows (each 10 arcsec wide) neighbouring the galaxy spectrum the intensity distribution of each column of the CCD frame (representing the spatial dimension) was fitted by a polynomial. By interpolating the fit functions over the rows of the galaxy spectrum a model image of the sky was created which then was subtracted from the raw image. In this way, the flux level of the background was reduced to a few percent of the galaxy's continuum level except for those regions that contained originally very strong emission lines. In Fig. 4 it can be seen that the sky level is about three times higher than the galaxy's flux at the $\rm Mg_{\it b}$ absorption line whereas this ratio is about ten at the Fe 5335 line. Nevertheless, even this line is well approximated by a fit using the superposition of five nearby elliptical galaxies of different line strengths (see below).

Extraction of the one-dimensional spectra was performed by an algorithm described by Horne (1986). Each row of the galaxy spectrum is weighted and added up in a way to achieve maximum signal–to–noise ratio for each pixel in the resulting one-dimensional spectrum. At the same time, cosmics are removed by analysing the profile perpendicular to the dispersion axis. Those pixel values that exceed the median of neighbouring pixels by more than a given threshold will be replaced by this median value. To determine the average signal–to–noise ratio of the whole spectrum its power spectrum was compared to synthesized noisy power spectra of a broadened comparison star. The observed galaxies have an S/N of 30 … 50 per Ångstrom after sky subtraction.

Kinematic parameters (radial velocities and velocity dispersions) of the distant elliptical galaxies were determined by two different methods. The first one was based on the Fourier correlation quotient (FCQ) analysis (Bender 1990). To check the reliability of the determined values the FCQ analysis was repeated using five different template stars of different spectral types and applied to different wavelength regions. The other method was a direct fitting procedure and was also applied to various parts of the galaxy spectrum. Here, essentially, several broadened spectra of either local ellipticals or stars were superposed on each other in a way to give an optimal fit to the spectrum. By systematically varying the broadening factor for the input spectra the velocity dispersion and its error could be estimated (for a detailed description see (Ziegler 1996)). All procedures were inspected visually and the results assigned a quality mark. In this way, the kinematic parameters were determined to an accuracy of about 10 per cent on average.

Line strengths of $\rm H_\beta$ (λ_0 = 4861 Å), $\rm Mg_{\it b}$ (λ_0 = 5173 Å), $\rm Mg_2$ ($\lambda_0 \approx$ 5175 Å; i.e. MgH+$\rm Mg_{\it b}$), Fe 5270 (λ_0 = 5269 Å) and Fe 5335 (λ_0 = 5328 Å) were measured according to the Lick system (Faber et al. 1985). However, only the $\rm Mg_{\it b}$ absorption line could be determined accurately; measurements of the other linestrengths are far less accurate, because these lines are affected by problems of sky subtraction and/or emission lines. With respect to $\rm H_\beta$ there is no means to correct for a possible contamination of the absorption by emission, because for most of the galaxies the emission line of [O III] (λ_0 = 5007), which is usually used for this correction, is redshifted to the B–band, a very strong telluric absorption band. The low $\rm H_\beta$ index of galaxy A20 of *Abell 370* (see Appendix A for the nomenclature) that shows [O III] in emission demonstrates the possibility that $\rm H_\beta$ might be partially filled by emission in the other galaxies. The absorption lines of Fe 5270 and Fe 5335 are in most cases rather noisy because they lie in that region of the spectrum which is dominated by very strong sky lines (see Fig. 4). Here, the residuals after sky subtraction are so large that they prevent any reliable measurement. This situation is worse for Fe 5335. In addition, there are several weak water bands so variable that they can not be corrected for with a spectrophotometric standard star. The same problem arises for $\rm Mg_2$, because its red continuum window coincides with the Fe 5335 line. In order to compare the linestrengths of the distant galaxies with the Lick system the effects of different spectral resolution, broadening by the velocity dispersion, and redshift had been taken into account. Absorption line strengths of galaxies with high velocity dispersion are systematically underestimated in the Lick system due to the fixed continuum windows. But this effect can easily be corrected by simulations with broadened template stars. The linestrengths of $\rm Mg_{\it b}$ and $\rm H_\beta$ of all observed galaxies are tabulated in Table B1. The $\rm Mg_{\it b}$ linestrengths could be determined to an accuracy of about 5 per cent on average.

The distant galaxies are so faint that all the observed light must be combined in a one-dimensional spectrum leading to mean values of the extracted parameters weighted by lu-

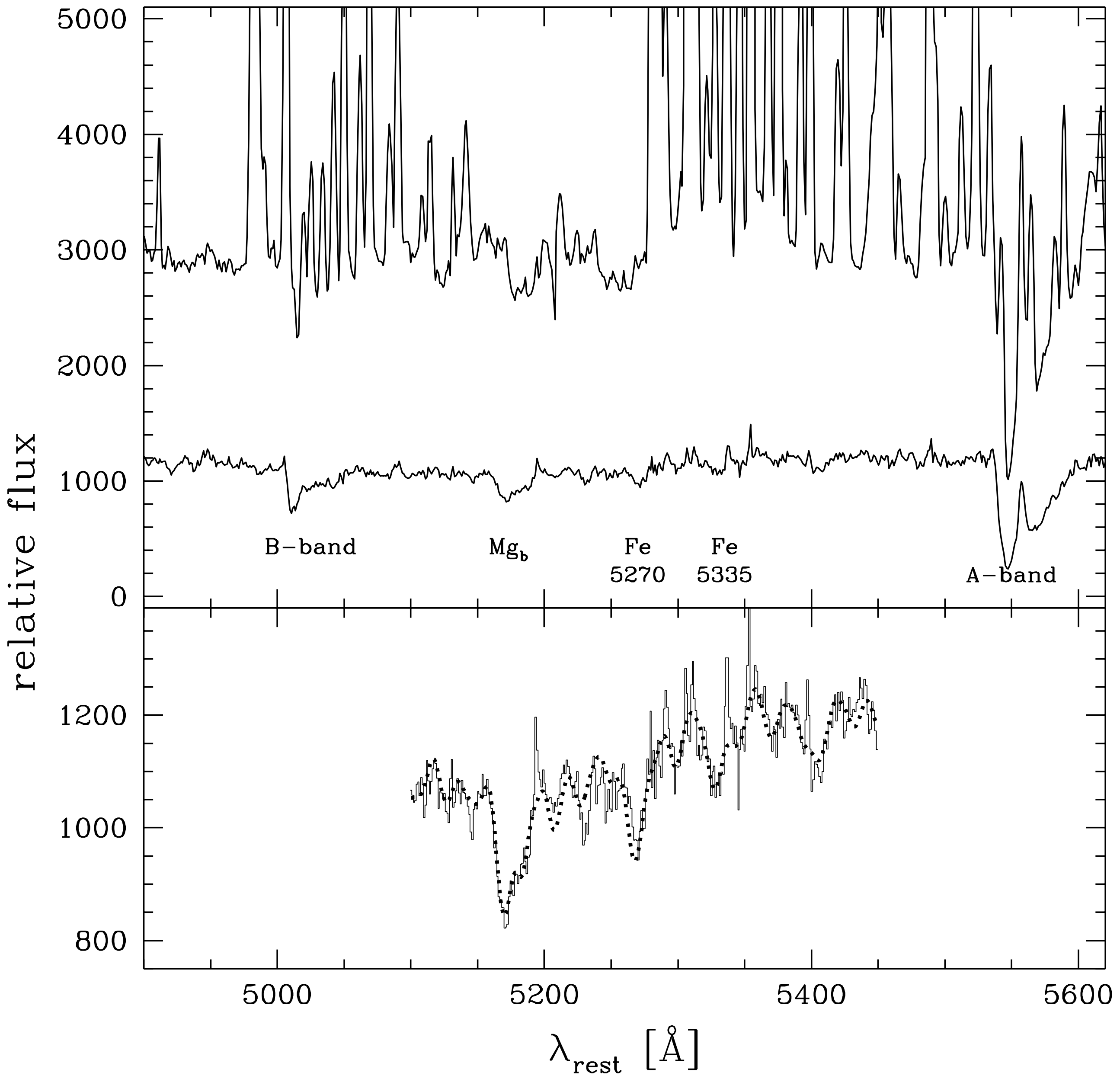

Figure 4. Upper panel: rest–frame spectra of an elliptical galaxy in the cluster *Abell 370* before and after sky subtraction. The Mg absorption around $\lambda_0 = 5170$ Å can be readily seen in the lower sky subtracted spectrum. (The features at $\lambda_0 \sim 5000$ and $\lambda_0 \sim 5550$ Å are the blueshifted atmospheric B- and A-band, resp.). Lower panel: fit (dotted line) to the galaxy spectrum using a superposition of spectra of nearby ellipticals.

minosity. Because elliptical galaxies have radial gradients in both velocity dispersion and linestrengths, the effect of different aperture size must be taken into account when comparing distant to local galaxies. A much larger part of the galaxy will be averaged for the distant ellipticals than for the nearby ones. Thus, the quasi-*integral* values of the $z = 0.37$ ellipticals must be transformed into quasi-*central* values as they have been observed for our comparison sample of Coma and Virgo ellipticals. To study the dependence of Mg$_b$ and σ on aperture size we made simulations with a model galaxy, the surface brightness of which followed the de Vaucouleurs law and assuming Mg$_b$ and σ to be constant along isophotes.

The mean values were calculated according to the following formula

$$\langle X \rangle \quad = \int_{aperture} I(r) X(r)\, dA \Bigg/ \int_{aperture} I(r)\, dA \; , \qquad (18)$$

with $I(r)$ and $X(r)$ being the radial profiles of the intensity and Mg$_b$ or $\log\sigma$, respectively, and A the total area of the aperture. Ideally, the functions Mg$_b(r)$ and $\log\sigma(r)$ should be determined from data of several ellipticals with r sampled out to at least five effective radii (r_e). In the case of Mg$_b$ we deduced the following profile based on a study of

114 elliptical galaxies out to about $3\,r_e$ (González & Gorgas 1995) (using equation (1) to transform Mg_2 into Mg_b):

$$\mathrm{Mg}_b = -0.87\,\mathrm{lg}(r/r_e) + c. \tag{19}$$

From a yet-unpublished investigation of nearby ellipticals by Saglia et al. with data out to $r \approx 2.5\,r_e$ we find the following profile for $\log\sigma$ to be

$$\mathrm{lg}\,\sigma(r) = -0.11\,(r/r_e)^{3/4} + c. \tag{20}$$

This profile falls off considerably steeper for large r_e than previously published profiles based on data with a smaller radial extent (e.g. Jørgensen, Franx, & Kjærgaard 1995). The power-law function of $\log\sigma(r)$ leads to a dependence of the aperture correction on the galaxy's effective radius whereas the correction is independent of r_e in the case of the logarithmic function of $\mathrm{Mg}_b(r)$. Both the input functions $X(r)$ and the determined profiles of the mean values $\langle X(\leq r)\rangle(r)$ are illustrated in Fig. 5. Because we can not determine the effective radii of all our distant galaxies accurately we chose a value of 30 arcsec as a first approximation in the present study (see Ziegler 1997 for the subsample with measured r_e from *HST* images). To transform our measured data of the distant ellipticals to the apparent diameters of Coma and Virgo ellipticals and the aperture size used for their observations (Dressler et al. 1987) we applied a mean aperture correction of $\Delta\,\mathrm{lg}\,\sigma = 0.042$ and $\Delta\mathrm{Mg}_b = 0.60$.
Using the same simulations we studied the influence on the aperture correction caused by the ellipticity of the galaxy (E0 – E7), the deviation of position angle from slit angle (0 – 90 degrees), the offset between galaxy center and slit position (0 – 2 arcsec) and the ratio of the sides of a rectangular slit (1 – ∞). It turned out that the variations of the aperture corrections amounted in the most cases only to $1-2$ per cent and could be therefore neglected. Only $\Delta\,\mathrm{lg}\,\sigma$ varied up to 10 per cent in extreme cases of high eccentricity or large misplacement of the slit.

6 RESULTS

6.1 The Mg_b–σ relation at $z \approx 0.37$ and the ages of elliptical galaxies

Here we present data of 21 elliptical galaxies in three clusters at nearly the same redshift: *MS 1512+36* ($z = 0.372$), *Abell 370* ($z = 0.375$) and *CL 0949+44* ($z = 0.377$). In Fig. 6, the distribution of the age and metallicity-dependent Mg_b index and the internal velocity dispersion (σ) of these galaxies, as well as of our comparison sample of nearby ellipticals in the Coma and Virgo cluster, is given. The distant ellipticals show a similar correlation between the two parameters like the local ones, but Mg_b is lower than the mean value of the comparison galaxies for any given σ. This can not be an artifact of our selection. The ellipticals of our sample in *Abell 370* have a colour cut-off $(B-V)_{\mathrm{obs}} > 1.4$ mag. Applying k–corrections (eqs. 12 and 14) the rest–frame cut-off is $(B-V)_{\mathrm{rest}} > 0.8$ mag. This colour criterion translates into a selection of our galaxies with respect to Mg_b and σ, when the tight correlations between $(B-V)$ colour and these parameters (Bender, Burstein, & Faber 1993) are considered together with equation (1):

$$(B-V)_0 = 1.12\,\mathrm{Mg}_2 + 0.615 \tag{21}$$

$$\Rightarrow \quad \mathrm{Mg}_{b,\mathrm{obs}} \geq 2.5\,\text{Å};$$

$$(B-V)_0 = 0.224\,\mathrm{lg}\,\sigma_0 + 0.429 \tag{22}$$

$$\Rightarrow \quad \mathrm{lg}(\sigma_{\mathrm{obs}}/(\mathrm{km\,s^{-1}})) \geq 1.65.$$

So, we should in principle be able to detect objects with Mg_b as weak as 2.5 Å. The absence of objects with high σ and low Mg_b is therefore significant and underlines the existence of an Mg_b–σ relation at $z = 0.37$.
The reduction of Mg_b with respect to the mean local relationship is weak but significant. A Student's T–test gives a significantly lower mean value for the distant sample than for the comparison sample. The mean reduction $\langle\Delta\mathrm{Mg}_b\rangle = -0.37$ Å with an error of the mean of 0.08 Å between $z = 0.37$ (corresponding to a look–back time $t_{\mathrm{lb}} \approx 5$ Gyr) and $z = 0$ is so low that it can be only understood, if the distant stellar populations are already old themselves. It is fully consistent with a purely passive evolutionary behaviour of elliptical galaxies since $z = 0.37$. Significant star bursts that would change the overall metallicity at a detectable level are ruled out because of the small evolution. Thus, equation (4) can be transformed to:

$$\frac{\mathrm{Mg}_b(z\!=\!0)}{\mathrm{Mg}_b(z)} = \left(\frac{\mathrm{age}\;(z\!=\!0)}{\mathrm{age}\;(z)}\right)^{0.15\ldots0.20}. \tag{23}$$

With the average values $\mathrm{Mg}_b(z\!=\!0) = 4.8$ Å and $\langle\Delta\mathrm{Mg}_b\rangle(z = 0.37) = -0.37$ Å, the distant galaxies have already $\approx 2/3$ the age of local ellipticals. Equation (23) in connection with the local Mg_b–σ relation (equation (2)) can be used to derive expected functions of $\mathrm{Mg}_b(\sigma, z\!=\!0.37)$ for different cosmologies (H_0, Ω_0) and redshifts of formation (z_f). In Fig. 6, the expected locations of Mg_b–σ at $z_{\mathrm{obs}} = 0.37$ are shown as hatched areas for $z_f = 1$ and 4, respectively, and any combination of $\Lambda = 0, q_0 = 0\ldots1, H_0 = 50\ldots100$ km s^{-1} Mpc^{-1} and $\partial\,\mathrm{lg}\,\mathrm{Mg}_b/\partial\,\mathrm{lg}\,t = 0.15\ldots0.20$. Comparing this with the observed values, it follows that the majority of the stars of most of the elliptical galaxies in clusters must have been formed at redshifts $z > 2$, those of the most luminous galaxies probably even at $z > 4$. The estimated age is probably a lower limit to the real formation era, because the applied aperture correction (arrow in Fig. 6) followed rather conservative assumptions on the gradients of Mg_b and σ (i.e. too-shallow gradients).
Given the large errorbars of our current data and the very low number of observed galaxies with low σ, it is rather speculative to comment on a possible change of the slope of the Mg_b–σ relation. Taking the data at face value it seems that the less massive ellipticals are younger than the more massive ones. This conclusion can not be circumvented by claiming that those galaxies with very low Mg_b for their σ are E+A galaxies that had one late starburst. Because of our colour selection, an E+A would enter our sample only 2 Gyr after its starburst when its $(B-V)$ colour returned to almost normal. At that time, the Mg_b index has also almost reached the value it had before the starburst. In fact, galaxy *A28* of *Abell 370* was put close to the E+A class on the basis of its high H_δ absorption (Henry & Lavery 1987), but both its Mg_b and H_β are like in normal ellipticals (see Figs. 6 and 7).
It was claimed recently, on the basis of observed higher values of H_β, that less luminous ellipticals could have younger mean ages than giants (Faber et al. 1995). Our distant galax-

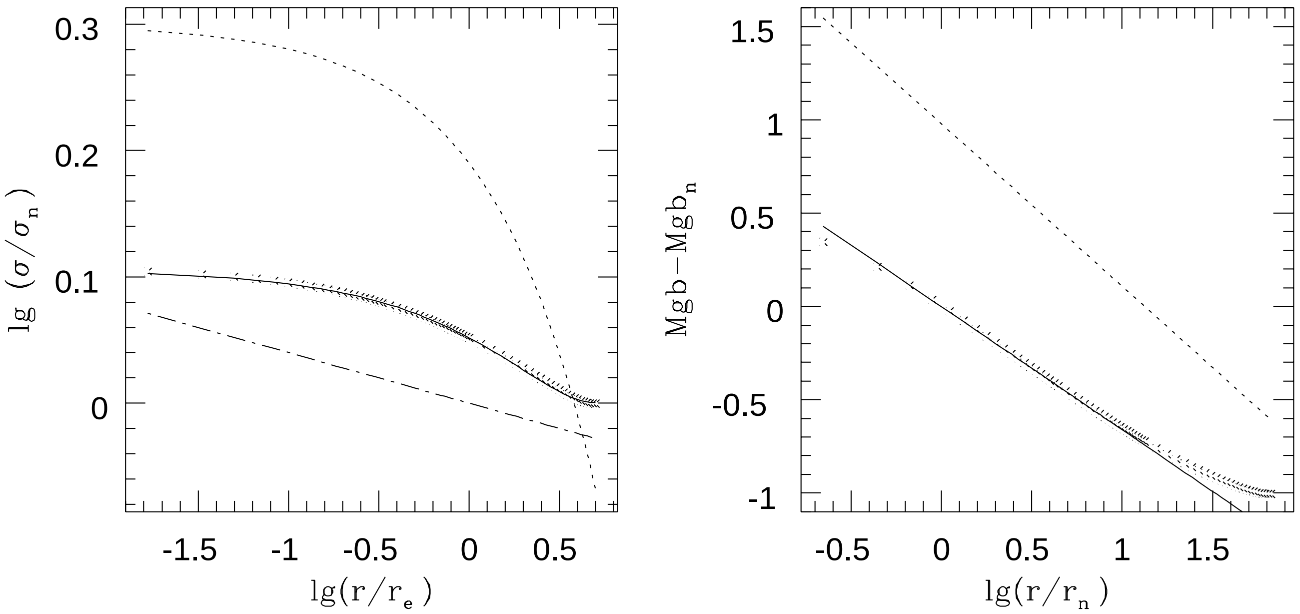

Figure 5. Radial profiles of the mean values for $\langle \lg \sigma \rangle$ (left panel) and $\langle \mathrm{Mg}_b \rangle$ (right panel) (see equation (18)): crosses = mean values as computed by the simulation; solid line = fit to these values; dotted line = radial gradient for $\lg \sigma$ (equation (20)) and Mg_b (equation (19)); dot-dashed line = logarithmic gradient for $\lg \sigma$ chosen by other authors.

ies do not show any correlation with the H_β index in the sense that the galaxies with very low Mg_b would have very high H_β. But remember the problems in determining H_β of the distant ellipticals as stated in Section 5.2. Also, we applied no aperture corrections to H_β, as nearby ellipticals are found to have nearly radially constant H_β (González 1993). Fig. 7 compares the H_β values of the distant ellipticals to the nearby sample. There is no significant difference between the two distributions and the outliers can be understood in terms of peculiarities of the spectra.

6.2 The Faber–Jackson relation at $z \approx 0.37$ and the luminosity evolution of elliptical galaxies

Stellar population models predict an evolution with age not only for absorption lines but also for the luminosity. For passively evolving simple stellar populations, the increase in brightness with redshift is most prominent in the B–band. Luminosity differences of elliptical galaxies can be well studied on the basis of the tight correlation between absolute blue magnitude (M_B) and velocity dispersion (Faber & Jackson 1976). The very small evolution found with the Mg_b–σ test excludes dissipative mergers that could substantially change σ between $z = 0.4$ and today. Non-dissipative mergers, that are not strictly ruled out in passive evolution models, do also not lead to any substantial change of the velocity dispersion (e.g. Aarseth & Fall 1980, Heyl, Hernquist, & Spergel 1996). Thus, the M_B of our distant galaxies can be directly compared to M_B of the comparison ellipticals at the same velocity dispersion. The determination of M_B as described in Section 5.1.1 depends first on the observational data (apparent magnitudes, aperture correction), second on the k–correction and third on the chosen cosmology and IMF. In the upper panel of Fig. 8 the data of the ellipticals at $z = 0.37$ (choosing $H_0 = 50\,\mathrm{km\,s^{-1}\,Mpc^{-1}}, q_0 = 0.5, \Lambda = 0$) are compared to data of Coma and Virgo ellipticals (Dressler et al. 1987). A principal components analysis of the Coma data yields, as the best fit,

$$M_B/\,\mathrm{mag} = -2.42 - 8\lg[\sigma/(\mathrm{km\,s^{-1}})]. \tag{24}$$

The distant ellipticals are on average significantly more luminous than the nearby ones as proven by a Student's t–test. The mean brightening in this example amounts to $\langle \Delta \mathrm{M}_B \rangle (z = 0.37) = -0.63 \pm 0.10\,\mathrm{mag}$. Now the question arises, whether this evolution of the luminosity is compatible with the results of the Mg_b–σ test. From stellar population synthesis models (Worthey 1994) for SSP's (Salpeter–IMF), we find a linear relationship between $\Delta \mathrm{M}_B$ and $\Delta \mathrm{Mg}_b$ which is well suited for ages greater than 1.5 Gyr and metallicities between half and twice solar,

$$\Delta \mathrm{M}_B/\,\mathrm{mag} \approx (1.4 \pm 0.1) \times \Delta \mathrm{Mg_b}/\text{Å}. \tag{25}$$

With this formula, the mean reduction of $\langle \Delta \mathrm{Mg}_b \rangle (z = 0.37) = -0.37 \pm 0.08\,\text{Å}$ translates into $\langle \Delta \mathrm{M}_B \rangle (z = 0.37) = -0.50 \pm 0.11\,\mathrm{mag}$. Thus, the amount of evolution of elliptical galaxies between $z = 0$ and $z = 0.37$ found with the Mg_b–σ test is in agreement with the brightening of the galaxies as derived from the Faber–Jackson relation for the chosen cosmology. Varying q_0 from 0.5 to 1 or 0 would change the absolute B magnitude of the observed ellipticals by ± 0.11 mag on average (remember that not only the luminosity distance is affected but also the effective radii and therefore the aperture correction). A change of the slope of the IMF by $\Delta x = \pm 1$ from the Salpeter value of $x = 1.35$ would result in a shift of the B magnitudes of ± 0.16 mag (equation (17)). Thus, the current data with their errors do not indicate an unusual IMF slope and are compatible with $q_0 = 0.5 \pm 0.5$. The above procedure can also be turned around. Then, for each galaxy the B magnitude is corrected for evolution according to its individual reduction of Mg_b with respect to

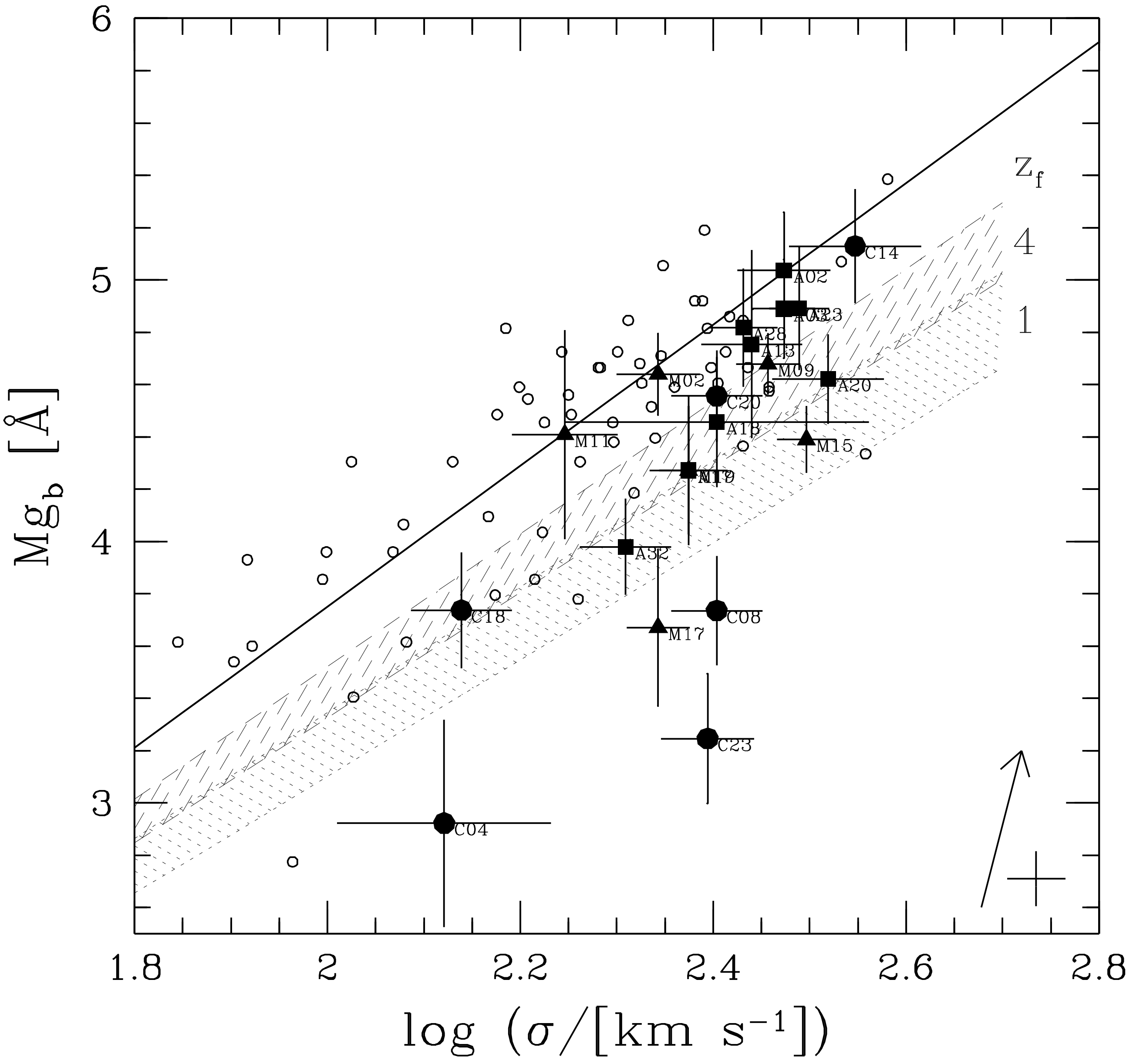

Figure 6. $\mathrm{Mg}_b - \sigma$ pairs at $z = 0.37$ (big symbols with errorbars, labels see Appendices) compared to the local Mg_b–σ relation (solid line: equation (2), small circles: Coma and Virgo ellipticals, typical errorbar in lower right corner). Arrow: aperture correction applied. Hatched areas: expected Mg_b–σ at $z_{\mathrm{obs}} = 0.37$ for $z_f = 1$ and 4, respectively, and different cosmologies and stellar population models.

the mean local Mg_b–σ relation using equation (25). The result of this individual correction for the luminosity evolution is shown in the lower panel of Fig. 8. In this case the distributions of the distant and local ellipticals are almost identical and even the slopes are very similar. This time, the average brightening amounts to $\langle \Delta \mathrm{M}_B \rangle (z = 0.37) = -0.50 \pm 0.14$ mag.

7 CONCLUSIONS

Comparing the Mg_b absorption line index of a sample of elliptical galaxies in three clusters at a redshift $z = 0.37$ with the local Mg_b–σ relation we find an average reduction $\langle \Delta \mathrm{Mg}_b \rangle = -0.37 \pm 0.08$ Å. This is evidence for significant but weak evolution of elliptical galaxies in clusters within a look–back time of ≈ 5 Gyr. It is compatible with the passive evolution of stellar population synthesis models (Worthey 1994, Bruzual & Charlot 1997). The mild evolution requires that the majority of the stellar population of normal cluster ellipticals was formed at redshifts $z_f > 2$. The most massive ellipticals might even have a mean formation redshift of $z_f > 4$. This implies that star formation happened already when the Universe was very young (for the standard cosmology $\Lambda = 0, q_0 = 0.5, H_0 = 50\,\mathrm{km\,s^{-1}\,Mpc^{-1}}$, $z = 4$ corresponds to $t_U = 1$ Gyr only). However, in the framework of CDM-dominated hierarchical clustering, giant ellipticals are assembled from smaller entities at much later times (Baugh,

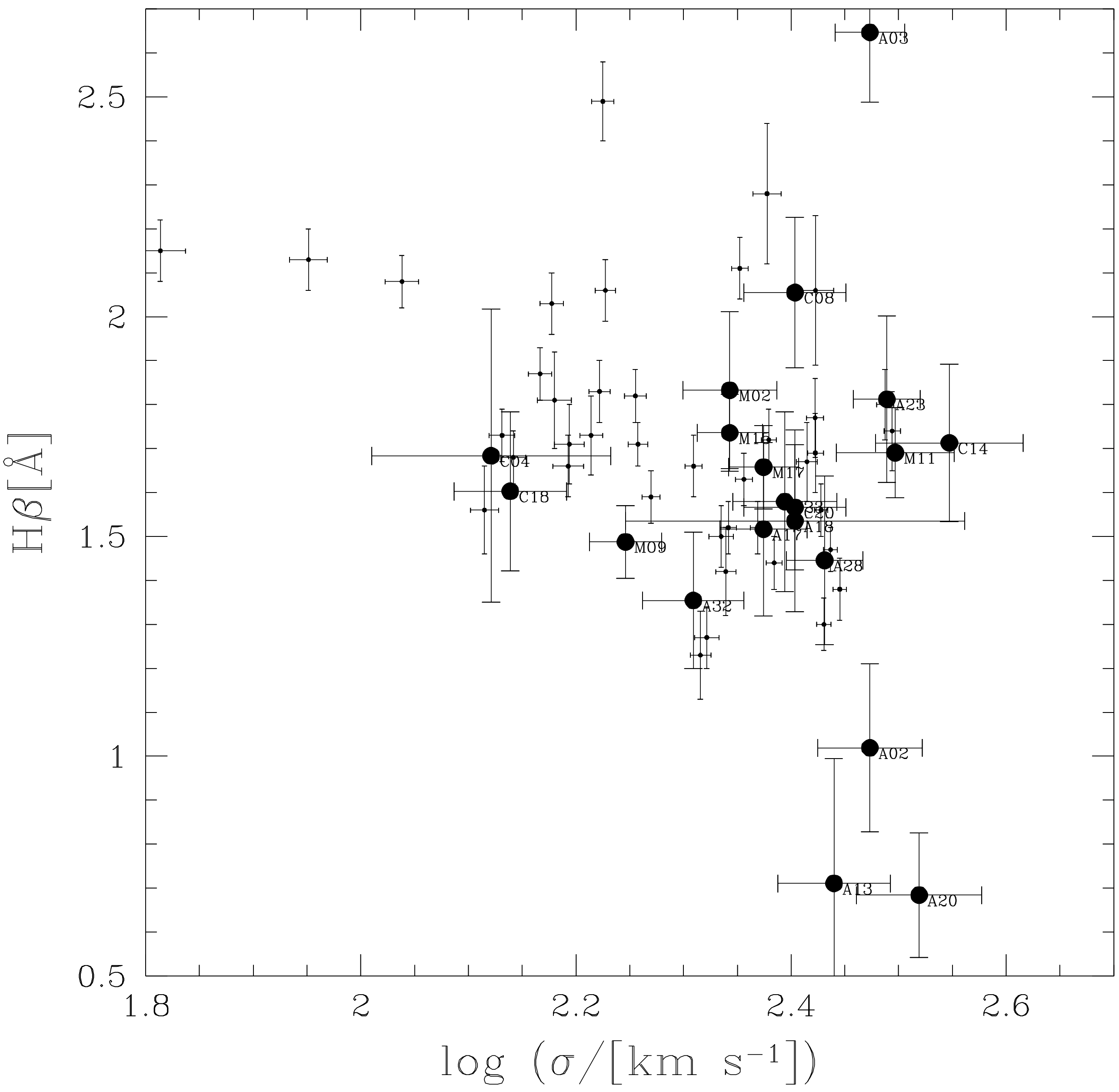

Figure 7. $H_\beta - \sigma$ pairs at $z = 0.37$ (big symbols with error bars, labels see Appendices) compared to nearby field ellipticals (small symbols, González 1993).

Cole, & Frenk 1996). In order to have, nevertheless, such a high mean stellar age, the merging of the protogalaxies to a very massive elliptical galaxy must have been essentially dissipationless, without any significant new star formation. The gas content of the merging haloes must therefore have been very low in comparison with their stellar mass. The normal mass ellipticals with mean stellar ages corresponding to $z_f = 2$ ($t_U = 2.5$ Gyr) on the other hand, could have their major star-forming phase at the time of their assembly. Such a scenario corresponds to the *gas/stellar continuum* model (Bender, Burstein, & Faber 1993): the gas content and, therefore, the role of dissipation of the last *major merger* decreases for increasing mass of the resultant galaxy. The epoch of formation derived here is also in agreement with semi-analytic CDM simulations, for which the last dissipative *major merger* leading to a giant elliptical occured at $z > 2$ (Kauffmann 1996). If the slope of the distant Mg_b–σ relation is different from the local one as marginally indicated by the present data then less luminous ellipticals would be systematically younger than the most luminous ones. This would agree with an H_β analysis of a sample of nearby ellipticals suggesting that the mean age of the stellar population gets younger with decreasing luminosity (Faber et al. 1995).

We showed that the weakening of the Mg_b index of cluster ellipticals at $z = 0.37$ corresponds to the brighten-

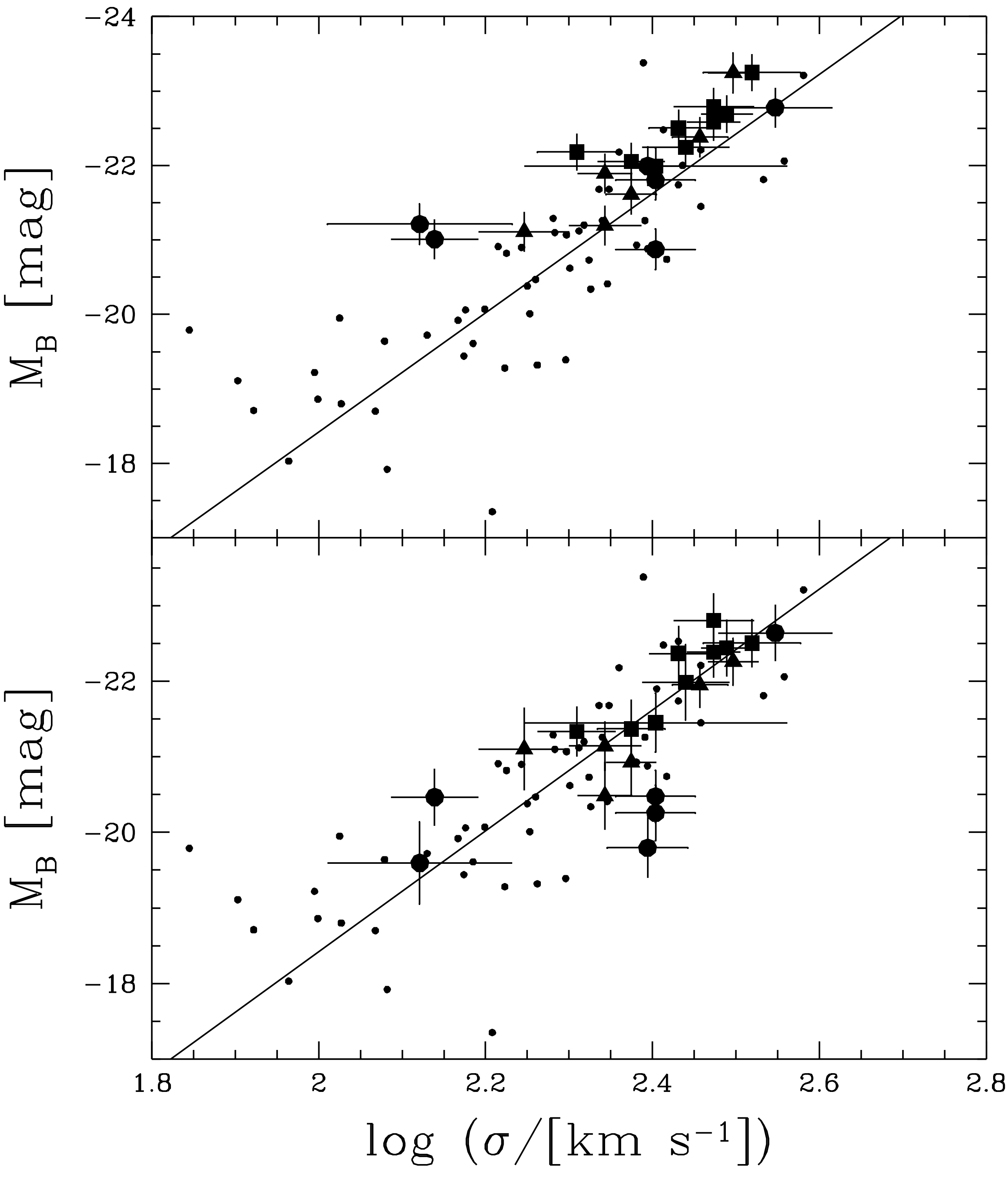

Figure 8. $M_B - \sigma$ pairs at $z = 0.37$ (big symbols with errorbars) compared to the local Faber–Jackson relation (solid line: (equation (24)), small circles: Coma and Virgo ellipticals). Upper panel: uncorrected absolute B magnitudes ($H_0 = 50\,\mathrm{km\,s^{-1}\,Mpc^{-1}}, q_0 = 0.5, \Lambda = 0$), lower panel: magnitudes of the distant ellipticals corrected for evolution as found by the Mg_b–σ test.

ing of the B luminosity by $\langle \Delta M_B \rangle = -0.50 \pm 0.14$ mag. This is in quantitative agreement with population synthesis of passively evolving galaxies. Our synthesized galaxy (using Bruzual & Charlot 1997 models) that matches the observed colours of ellipticals in *Abell370* (see Section 5.1.1: k–correction) experiences an evolution of the rest–frame B magnitude of $\Delta M_B = -0.61$ mag. It is also consistent with results obtained by other groups. Schade et al. (1996) find, e.g., an increase of the blue luminosity by $\Delta M_{AB}(B) = -0.55 \pm 0.12$ mag for early-type galaxies in the cluster *MS 1621+26* at $z = 0.43$ and Barrientos, Schade, & López–Cruz (1996) $\Delta M_B = -0.64 \pm 0.3$ mag in the cluster *CL 0939+47* at $z = 0.41$.

The agreement of the evolutionary effects as found via the Mg_b–σ relation and the Faber–Jackson relation strongly supports the hypothesis that the stellar populations of elliptical galaxies, in the density environment of clusters of galaxies, formed very early and in a short period of time, with no substantial new star formation between $z = 0.4$ and today. This result is not biased in the sense that we would have chosen only that (small) fraction of the whole population of elliptical galaxies that *is* old (for a discussion see, e.g. Franx & van Dokkum 1996), because our selection criterion did not pick up only the reddest members. The rest–frame $(B - V)$ colour cut-off of 0.8 mag is well below the mean value for samples of nearby early-type galaxies. Of course, a much bigger sample is needed to clarify this issue in detail with selection based on spectroscopic criteria and not on colours. Another aspect to be studied in the future is the possible dependence of the Mg_b–σ relation on the density environment (de Carvalho & Djorgovski 1992, Lucey 1995, Jørgensen 1997). The three clusters investigated in this paper do have different richnesses but the small number of observed galaxies does not allow us to draw statistically significant conclusions about any dependence on density environment. The cluster with the biggest number of observed galaxies, *Abell370*, has a similar richness class like our local comparison cluster, Coma.

In a follow-up paper, we combine the individual evolutionary corrections as found via the Mg_b–σ relation with a full fundamental plane analysis of our HST images of the three clusters to calibrate elliptical galaxies as standard candles for the determination of the cosmological de-/acceleration parameter q_0 (Bender et al. 1997). Preliminary results are given in Bender, Saglia, & Ziegler (1996).

ACKNOWLEDGMENTS

The authors would like to thank Dr. G. Bruzual for his continous support with his models as well as Drs. R. P. Saglia, P. Belloni, L. Greggio and U. Hopp for many fruitful discussions. This work was supported by the "Sonderforschungsbereich 375–95 für Astro–Teilchenphysik der Deutschen Forschungsgemeinschaft" and by DARA grant 50 OR 9608 5.

REFERENCES

Aarseth, S. J., Fall, S. M. 1980, ApJ, 236, 43
Aragón–Salamanca, A., Ellis, R. S., Couch, W. J., Carter, D. 1993, MNRAS, 262, 764
Barnes, J. E., Hernquist, L. 1992, ARA&A, 30, 705
Barrientos, L. F., Schade, D., López–Cruz, O. 1996, ApJ, 460, L89
Baugh, C. M., Cole, S., Frenk, C. S. 1996, MNRAS, 283, 1361
Bender, R. 1990, A&A, 229, 441
Bender, R., Surma, P., Döbereiner, S., Möllenhoff, C., Madejsky, R. 1989, A&A, 217, 35
Bender, R., Burstein, D,, Faber, S. M. 1993, ApJ, 411, 153
Bender, R., Saglia, R. P., Gerhard, O. E. 1994, MNRAS, 269, 785
Bender, R., Ziegler, B., Bruzual, G. 1996, ApJ, 463, L51.
Bender, R., Saglia, R. P., Ziegler, B. 1996, in Bergeron, J. et al., eds, The Early Universe with the VLT. Springer, Berlin, in press, astro–ph/9608081
Bender, R., Saglia, R. P., Ziegler, B., Belloni, P., Bruzual, G., Greggio, L., Hopp, U. 1997, ApJ, in press
Bessell, M. S. 1983, PASP, 95, 480
Bower, R., Lucey, J. R., Ellis, R. S. 1992, MNRAS, 254, 601
Bruzual, G. 1996, in Bender, R., Davies, R., eds., Proc. IAU Symp. 171, New Light on Galaxy Evolution. Kluwer, Dordrecht, p. 61
Bruzual, G. A., Charlot, S. 1993, ApJ, 405, 538
Bruzual, G. A., Charlot, S. 1997, ApJ, in preparation
Burstein, D., Faber, S. M., Gaskell, C. M., Krumm, N. 1984, ApJ, 287, 586
Burstein, D., Heiles, Carl 1984, ApJS, 54, 33
Butcher, H., Oemler Jr., A., Wells, D. C. 1983, ApJS, 52, 183
de Carvalho, R. R., Djorgovski, S. 1992, ApJ, 389, L49
de Vaucouleurs, G. 1962, in McVittie, G. C., ed, Proc. IAU Symp. 15, Problems of Extra–Galactic Research. Macmillan, New York, p. 3
Dressler, A., Gunn, J. E. 1992, ApJS, 78, 1
Dressler, A., Lynden–Bell, D., Burstein, D., Davies, R. L., Faber, S. M., Terlevich, R. J., Wegner, G. 1987, ApJ, 313, 42
Dressler, A., Oemler Jr., A., Butcher, H. R., Gunn, J. E. 1994, ApJ, 430, 107
Ellis, R. S., Colless, M., Broadhurst, T., Heyl, J., Glazebrook, K. 1996, MNRAS, 280, 235
Elston, R., Silva, D. 1992, AJ, 104, 1360
Faber, S. M., Jackson, R. E. 1976, ApJ, 204, 668
Faber, S. M., Friel, E. D., Burstein, D., Gaskell, C. M. 1985, ApJS, 57, 711
Faber, S. M., Trager, S. C., González, J. J., Worthey, G. 1995, in van der Kruit, P. C., Gilmore, G., eds, Proc. IAU Symp. 164, Stellar Populations. Kluwer, Dordrecht, p. 249
Franx, M., van Dokkum, P. G. 1996, in Bender, R., Davies, R., eds., Proc. IAU Symp. 171, New Light on Galaxy Evolution. Kluwer, Dordrecht, p. 233
Freedman, W. L. 1992, AJ, 104, 1349
Glazebrook, K., Peacock, J. A., Miller, L., Collins, C. A. 1995, MNRAS, 275, 169
González, J. J. 1993, PhD thesis, University of California, Santa Cruz
González, J. J., Gorgas, J. 1995, in Buzzoni, A., Renzini, A., Serrano, A., eds, ASP Conference Series 86, Fresh Views on Elliptical Galaxies. ASP, p. 225
Henry, J. P., Lavery, R. J. 1987, ApJ, 323, 473
Heyl, J. S., Hernquist, L., Spergel, D. N. 1996, ApJ, 463, 69
Horne, K. 1986, PASP, 98, 609
Jørgensen, I. 1997, MNRAS, 288, 161
Jørgensen, I., Franx, M., Kjærgaard, P. 1995, MNRAS, 276, 1341
Kauffmann, G. 1996, MNRAS, 281, 487
Kauffmann, G., Charlot, S., White, S. D. M. 1997, MNRAS, 283, L117
Kelson, D. D., van Dokkum, P. G., Franx, M., Illingworth, G. D., Fabricant, D. 1997, ApJ, 478, L13
Larson, R. B. 1975, MNRAS, 173, 671

Table A3. Photometric data of galaxies with spectra in *MS 1512+36*

ID	X	Y	V	R	I	V–R	V–I
M02	328.6	489.2	21.74	20.40	19.40	1.34	2.34
M09	574.0	585.7	21.02	19.79	18.70	1.23	2.32
M11	592.8	521.4	21.38	20.16	18.97	1.22	2.41
M15	788.7	292.3	20.47	19.31	18.29	1.16	2.18
M17	807.3	548.9	20.94	19.82	18.77	1.12	2.17
M19	835.5	333.9	21.49	20.23	19.31	1.26	2.18

Lilly, S. J., Tresse, L., Hammer, F., Crampton, D., Le Fèvre, O. 1995, ApJ, 455, 108

Lucey, J. R. 1995, in van der Kruit, P. C., Gilmore, G., eds, Proc. IAU Symp. 164, Stellar Populations. Kluwer, Dordrecht, p. 281

Mattig, W. 1958, Astron. Nachr., 284, 109

Mellier, Y., Soucail, G., Fort, B., Mathez, G. 1988, A&A, 199, 13

Pahre, M. A., Djorgovski, S., de Carvalho, R. R. 1996, ApJ, 456, L79

Pickles, A. J., van der Kruit, P. C. 1991, A&AS, 91, 1

Rich, R. M., Mould, J. R. 1991, AJ, 101, 1286

Schade, D., Carlberg, R. G., Yee, H. K. C., Lopéz–Cruz, O., Ellingson, E. 1996, ApJ, 464, L63

Schade, D., Barrientos, L. F., Lopéz–Cruz, O. 1997, ApJ, 477, L17

Schmidt, M. 1968, ApJ, 151, 393

Schweizer, F. 1990, in Wielen, R., ed, Dynamics and Interactions of Galaxies. Springer, Heidelberg, p. 60

Stanford, S. A., Eisenhardt, P. R. M., Dickinson, M. 1995, ApJ, 450, 512

Steidel, C. C., Giavalisco, M., Pettini, M., Dickinson, M., Adelberger, K. L. 1996, ApJ, 462, L17

Tinsley, B. M. 1980, Fund. of Cosmic Physics, 5, 287

Toomre, A. 1977, in Tinsley, B. M., Larsen, R. B., eds, The Evolution of Galaxies and Stellar Populations. Yale Univ. Press, New Haven, p. 401

van Dokkum, P. G., Franx, M. 1996, MNRAS, 281, 985

Worthey, G. 1994, ApJS, 95, 107

Ziegler, B. 1996, PhD thesis, Universität Heidelberg

Ziegler, B. 1997, in da Costa, L. et al., eds, Galaxy Scaling Relations: Origins, Evolution and Applications. Springer, Heidelberg, in press, astro–ph/9701084

APPENDIX A: PHOTOMETRIC DATA

Contour plots of the clusters *Abell 370*, *CL 0949+44* and *MS 1512+36* are shown with the observed objects marked (Figs. A1, A2 and A3). North is up and east is left. *Abell 370* was observed with the ESO NTT using the EMMI focal reducer with a spatial resolution of 0.268 arcsec pixel^{-1} and a field of view of $\sim$ 9 x 9 arcmin^2. *CL 0949+44* and *MS 1512+36* were observed with the 2.2m-telescope on Calar Alto using a CCD camera at the Cassegrain focus with a spatial resolution of 0.281 arcsec pixel^{-1} and a field of view of $\sim$ 4.5 x 4.5 arcmin^2. Tables A1–A3 give magnitudes in the standard Kron–Cousins filter system (Bessell 1983).

APPENDIX B: SPECTROSCOPIC DATA

Spectra (Figs. B1–B7) and tables (Tables B1 and B2) with data relevant for the Mg_b–σ relation and Faber–Jackson relation are given. All spectra were taken with the 3.5m-telescope on Calar Alto with the TWIN spectrograph and cover the wavelength range $\lambda\lambda = 6500 - 7500$ Å. The instrumental resolution was 105 km s^{-1}. The absorption lines of H_β ($\lambda_0 = 4861$ Å), Mg_b ($\lambda_0 \approx 5173$ Å), Fe5270 ($\lambda_0 = 5269$ Å) and Fe5335 ($\lambda_0 = 5328$ Å) are readily visible in Figs. B1–B7 as is the telluric B–band ($\lambda_0 \approx 6900$ Å).

This paper has been produced using the Royal Astronomical Society/Blackwell Science LaTeX style file.

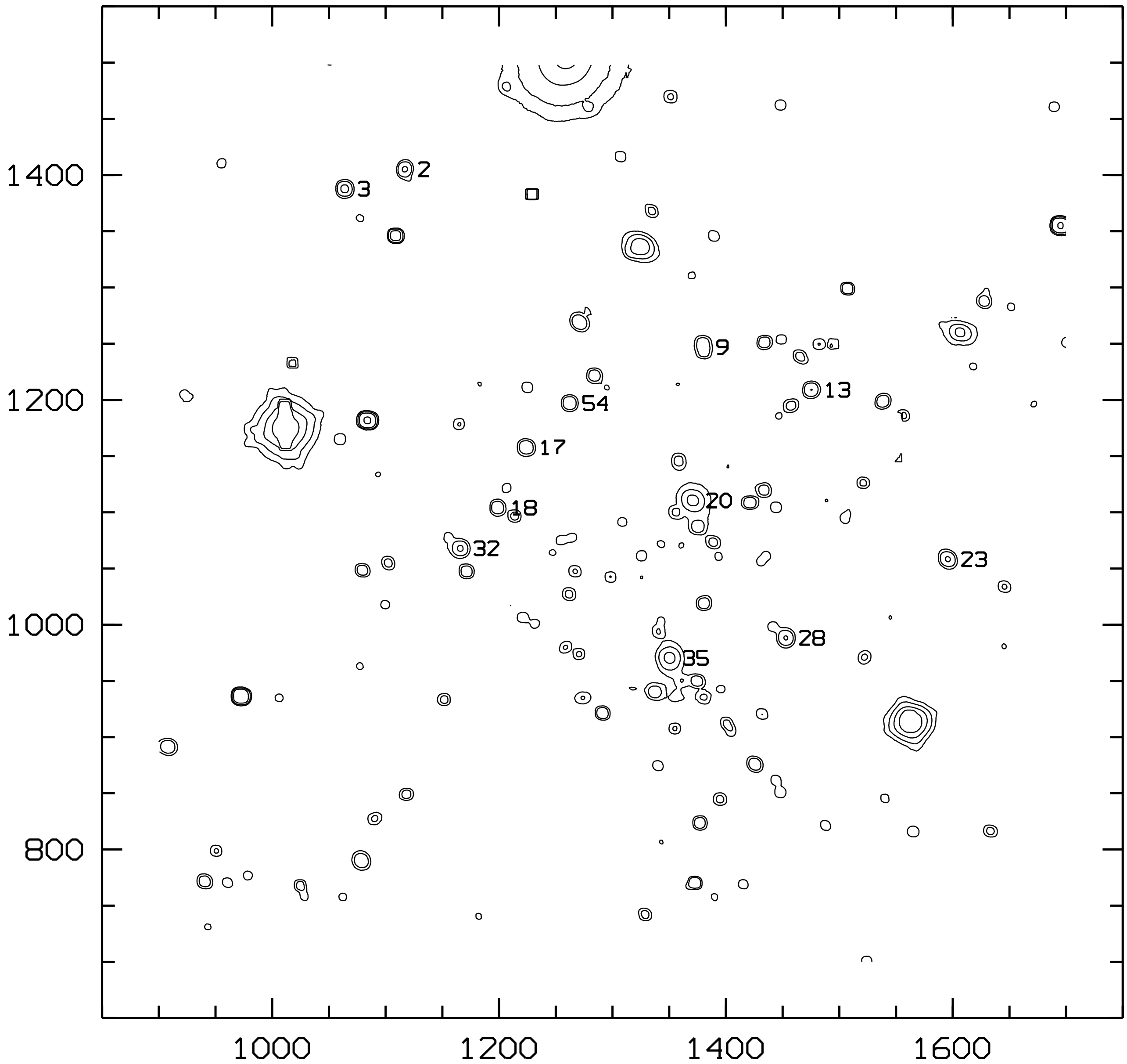

Figure A1. *Abell 370* at $z = 0.375$. Coordinates are CCD pixels and correspond to columns X and Y of Table A1. Labels follow column ID.

Table A1. Photometric data of galaxies with spectra in *Abell 370*.

ID	BOW	PK	X	Y	V	R	I	V–R	V–I
A02	31	132	1116.8	1405.2	20.01	18.93	18.17	1.08	1.85
A03	22		1063.7	1387.9	20.22	19.09	18.28	1.13	1.94
A13	34	107	1475.2	1209.2	20.42	19.19	18.41	1.23	2.01
A17	26	97	1223.9	1157.9	20.40	19.19	18.40	1.21	2.00
A18	41	88	1198.6	1104.2	20.55	19.42	18.63	1.13	1.90
A20	10	90	1370.9	1110.6	19.77	18.56	17.76	1.21	2.01
A23	21	70	1595.6	1058.3	20.18	19.04	18.22	1.14	1.96
A28	29	53	1452.8	988.3	20.13	19.06	18.25	1.07	1.88
A32		76	1165.7	1067.9	20.13	19.02	18.20	1.11	1.93

ID numbers correspond to the reference number of Table 1 in Mellier et al. (1988), BOW is the reference number of Table 3 in Butcher, Oemler Jr., & Wells (1983), while PK is the reference number of Table 4b in Pickles & van der Kruit (1991).

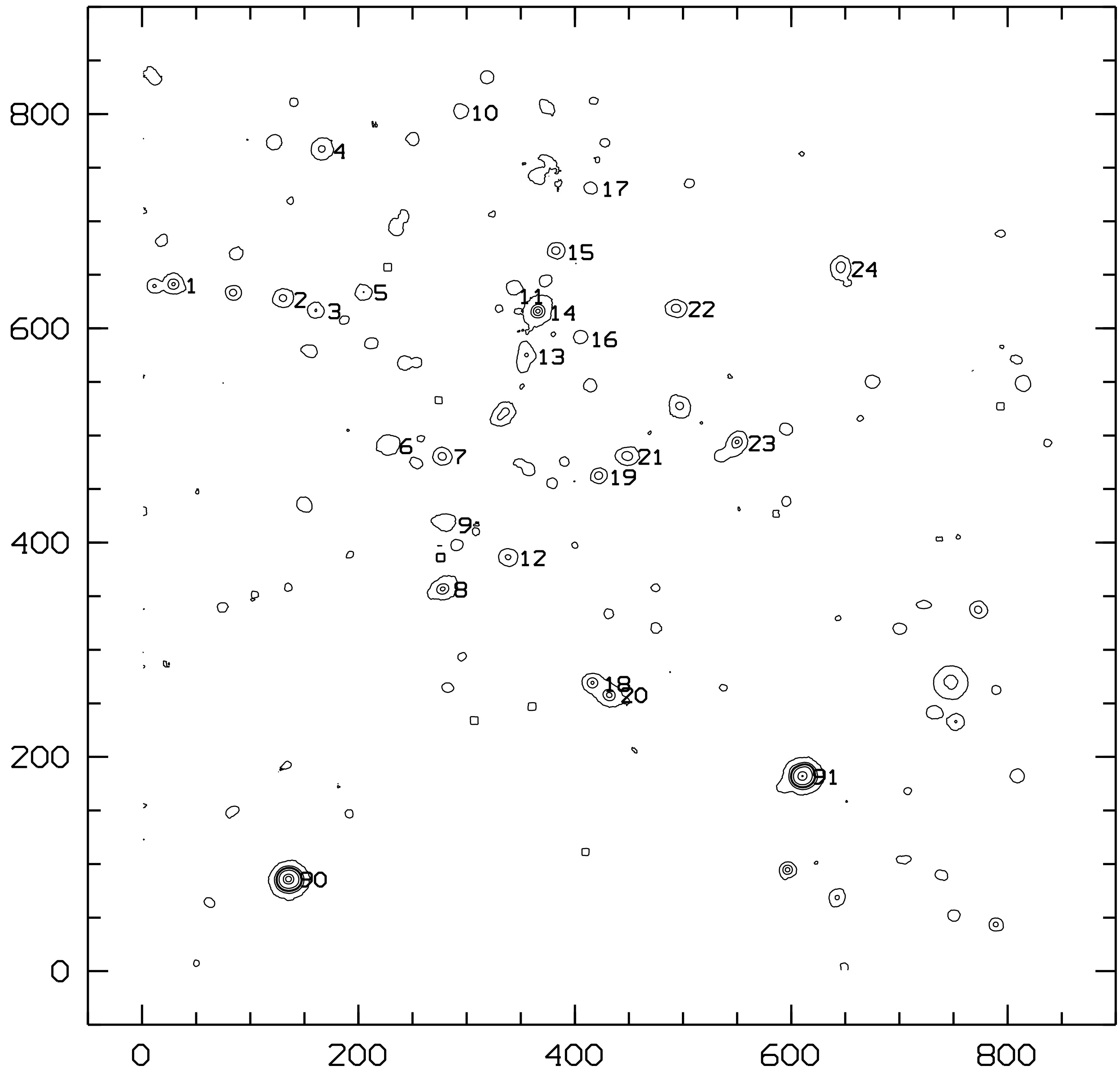

Figure A2. *CL 0949+44* at $z = 0.377$. Coordinates are CCD pixels and correspond to columns X and Y of Table A2. Labels follow column ID.

Table A2. Photometric data of galaxies with spectra in *CL 0949+44*

ID	DG	X	Y	V	R	I	V–R	V–I
C04	80	164.8	765.5	20.95	19.90	18.60	1.05	2.35
C08	193	276.7	356.2	20.81	19.43	18.71	1.38	2.10
C14	118	364.4	614.6	20.52	19.20	17.99	1.32	2.53
C18	217	414.7	268.1	21.16	20.31	18.83	0.85	2.33
C20	221	430.5	257.6	21.74	19.81	18.47	1.93	3.27
C23		548.2	492.7	20.59	19.67	18.43	0.92	2.16

DG is the reference number of Table 2 in Dressler & Gunn (1992).

Table B1. Spectroscopic data

ID	v_r	σ	$\Delta\sigma$	$\lg\sigma$	Mg_b	$Mg_{b,cor}$	ΔMg_b	$\Delta Mg_{b,evo}$	H_β	ΔH_β	$H_{\beta,cor}$
A02	108994	270	30	2.47	3.91	5.04	0.23	0.01	1.18	0.19	1.02
A03	108019	270	20	2.47	3.78	4.89	0.19	–0.14	2.75	0.16	2.65
A13	113224	250	30	2.44	3.73	4.75	0.36	–0.18	0.88	0.28	0.71
A17	114537	215	20	2.37	3.38	4.27	0.25	–0.49	1.68	0.20	1.52
A18	112877	230	80	2.40	3.51	4.46	0.25	–0.38	1.69	0.21	1.53
A20	113350	300	40	2.52	3.45	4.62	0.17	–0.53	0.85	0.14	0.68
A23	110390	280	20	2.49	3.75	4.89	0.23	–0.18	1.94	0.19	1.81
A28	111275	245	20	2.43	3.80	4.82	0.23	–0.10	1.60	0.19	1.45
A32	110591	185	20	2.31	3.18	3.98	0.18	–0.60	1.52	0.15	1.35
C04	104170	120	30	2.12	2.26	2.92	0.40	–1.15	1.86	0.33	1.68
C08	113600	230	25	2.40	2.86	3.74	0.21	–1.10	2.20	0.17	2.05
C14	114560	320	50	2.55	3.81	5.13	0.22	–0.10	1.83	0.18	1.71
C18	112860	125	15	2.14	3.05	3.74	0.22	–0.39	1.78	0.18	1.60
C20	113090	230	25	2.40	3.61	4.56	0.17	–0.28	1.72	0.14	1.57
C23	114010	225	25	2.39	2.42	3.25	0.25	–1.57	1.73	0.20	1.58
M02	111655	200	20	2.34	3.76	4.64	0.16	–0.04	1.99	0.18	1.83
M09	111514	260	20	2.46	3.63	4.68	0.12	–0.30	0.85	0.08	-1.07
M11	111807	160	20	2.25	3.63	4.41	0.40	–0.01	1.66	0.10	1.49
M15	111868	285	20	2.50	3.30	4.40	0.13	–0.70	1.82	0.09	1.69
M17	109135	200	15	2.34	2.86	3.67	0.30	–1.01	1.90	0.09	1.74
M19	110515	215	15	2.37	3.38	4.27	0.28	–0.49	1.81	0.24	1.66

ID refers to Tables A1, A2 and A3, v_r is the measured radial velocity in km s^{-1} (with an average error of $\approx \pm 20$ km s^{-1}), σ the measured velocity dispersion in km s^{-1}, $\Delta\sigma$ the error thereof, $\lg\sigma$ the decimal logarithm of the aperture corrected velocity dispersion, Mg_b the measured Mg_b linestrength in Å, $Mg_{b,cor}$ the Mg_b linestrength corrected for velocity dispersion and aperture, ΔMg_b the error thereof, $\Delta Mg_{b,evo}$ the evolution of Mg_b linestrength between $z = 0$ and $z = 0.37$, H_β the measured H_β linestrength in Å, ΔH_β the error thereof and $H_{\beta,cor}$ the H_β linestrength corrected for velocity dispersion.

Table B2. Absolute B–magnitudes ($H_0 = 50$ km s^{-1} Mpc^{-1}, $q_0 = 0.5$.)

ID	V_{tot}	ΔV	M_B	$\Delta M_{B,evo}$	$M_{B,cor}$	$\Delta M_{B,cor}$
A02	19.35	0.26	–22.79	–0.01	–22.80	0.36
A03	19.56	0.26	–22.58	0.19	–22.39	0.33
A13	19.90	0.26	–22.25	0.26	–21.99	0.49
A17	20.09	0.26	–22.05	0.68	–21.37	0.38
A18	20.16	0.26	–21.99	0.53	–21.45	0.38
A20	18.90	0.26	–23.25	0.74	–22.50	0.32
A23	19.45	0.26	–22.69	0.25	–22.44	0.37
A28	19.64	0.26	–22.50	0.13	–22.37	0.37
A32	19.96	0.26	–22.18	0.84	–21.33	0.33
C04	20.93	0.27	–21.21	1.61	–19.60	0.54
C08	20.34	0.27	–21.80	1.54	–20.26	0.36
C14	19.37	0.27	–22.78	0.13	–22.64	0.37
C18	21.14	0.27	–21.01	0.54	–20.46	0.37
C20	21.27	0.27	–20.87	0.39	–20.48	0.34
C23	20.15	0.27	–21.99	2.19	–19.80	0.40
M02	20.95	0.27	–21.20	0.05	–21.14	0.32
M09	19.77	0.27	–22.38	0.42	–21.95	0.30
M11	21.03	0.27	–21.11	0.01	–21.10	0.55
M15	18.90	0.27	–23.24	0.98	–22.26	0.31
M17	20.25	0.27	–21.89	1.40	–20.49	0.44
M19	20.53	0.27	–21.61	0.68	–20.93	0.43

ID refers to Tables A1, A2 and A3, V_{tot} is the total apparent V magnitude, ΔV the error thereof, M_B the absolute B magnitude in the rest-frame of the galaxy, $\Delta M_{B,evo}$ the evolutionary correction according to equation 25, $M_{B,cor}$ the absolute B magnitude corrected for evolution and $\Delta M_{B,cor}$ the error thereof.

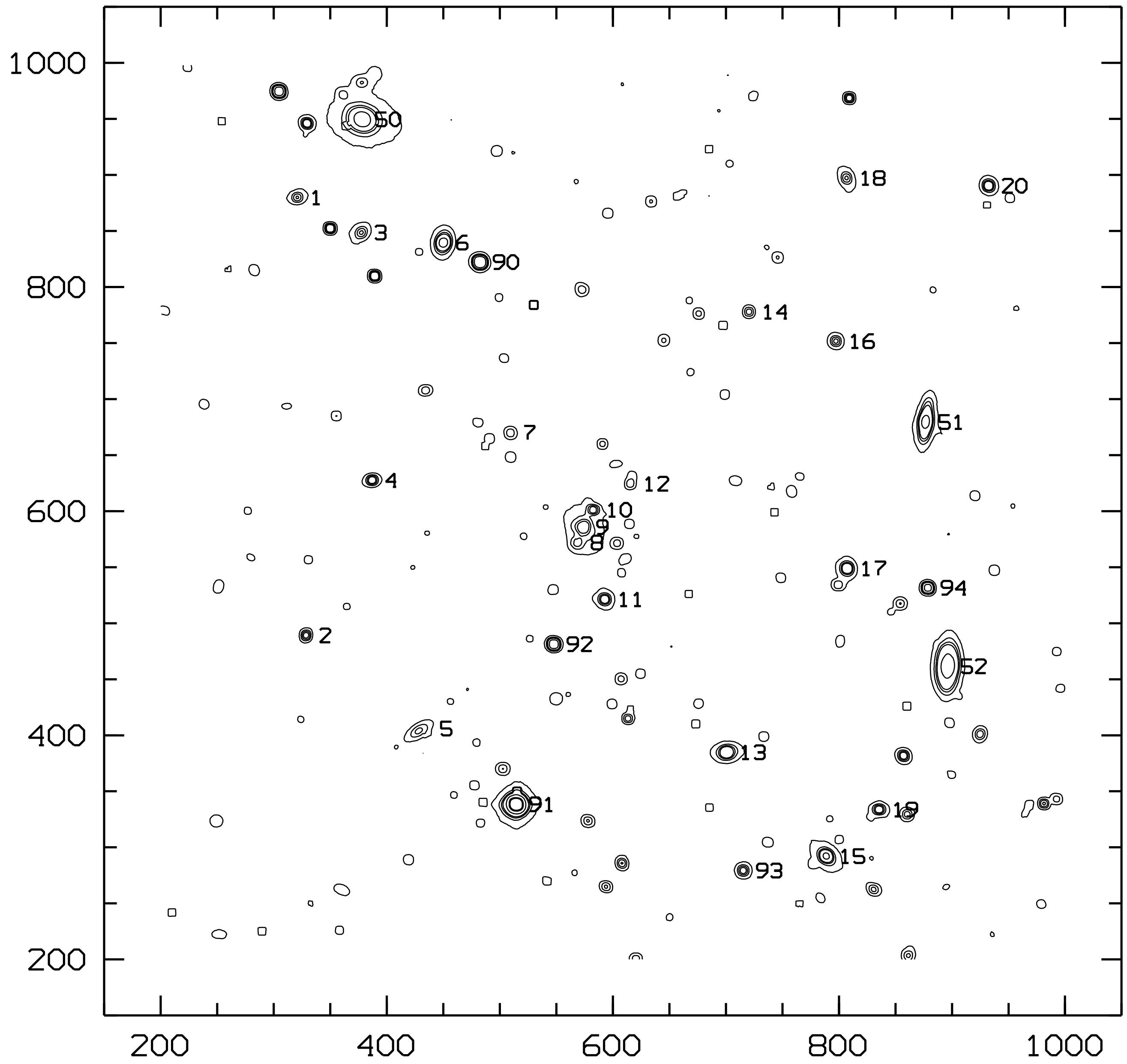

Figure A3. *MS 1512+36* at $z = 0.372$. Coordinates are CCD pixels and correspond to columns X and Y of Table A3. Labels follow column ID.

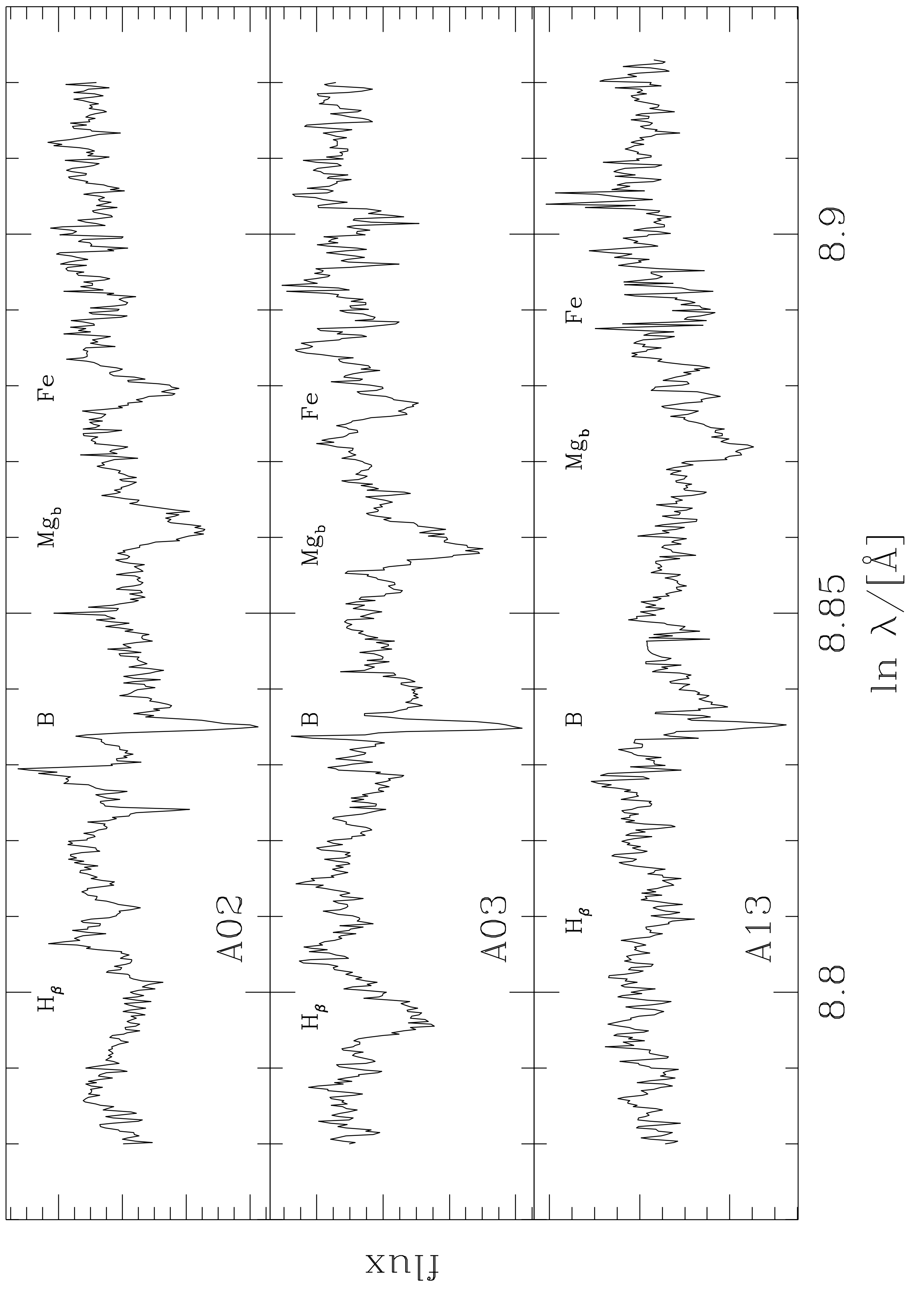

Figure B1. Spectra of galaxies A02, A03 and A13.

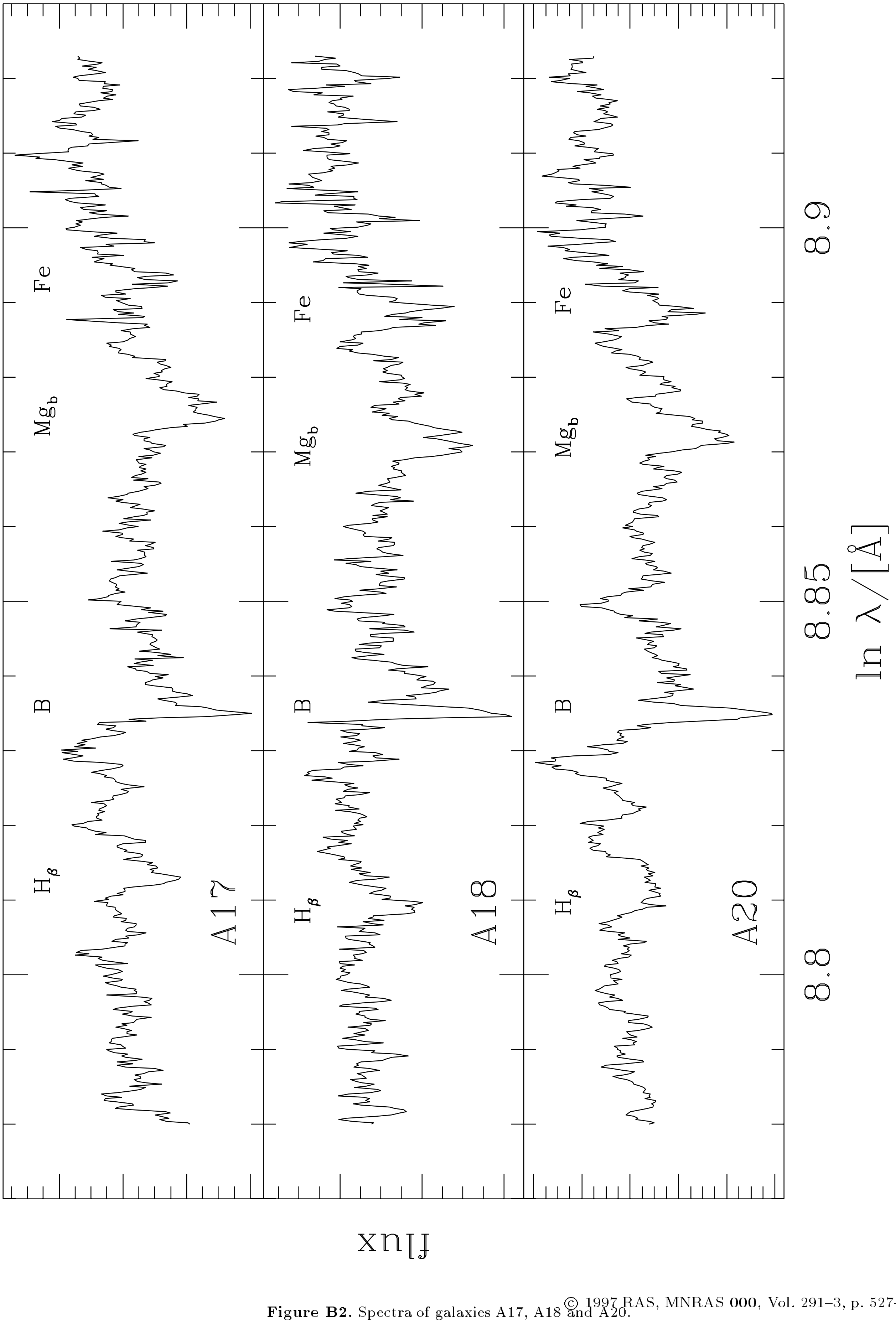

Figure B2. Spectra of galaxies A17, A18 and A20.

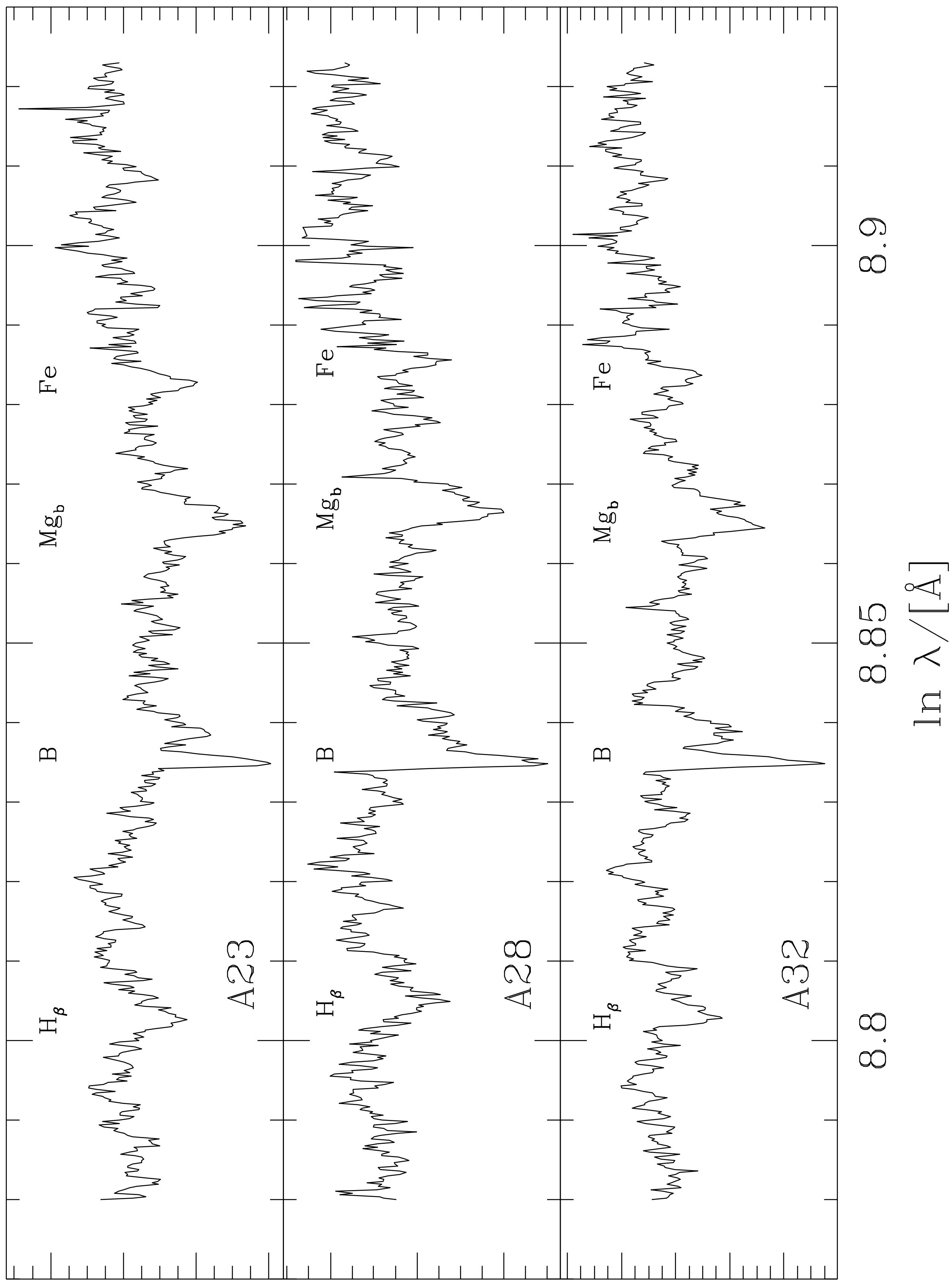

Figure B3. Spectra of galaxies A23, A28 and A32.

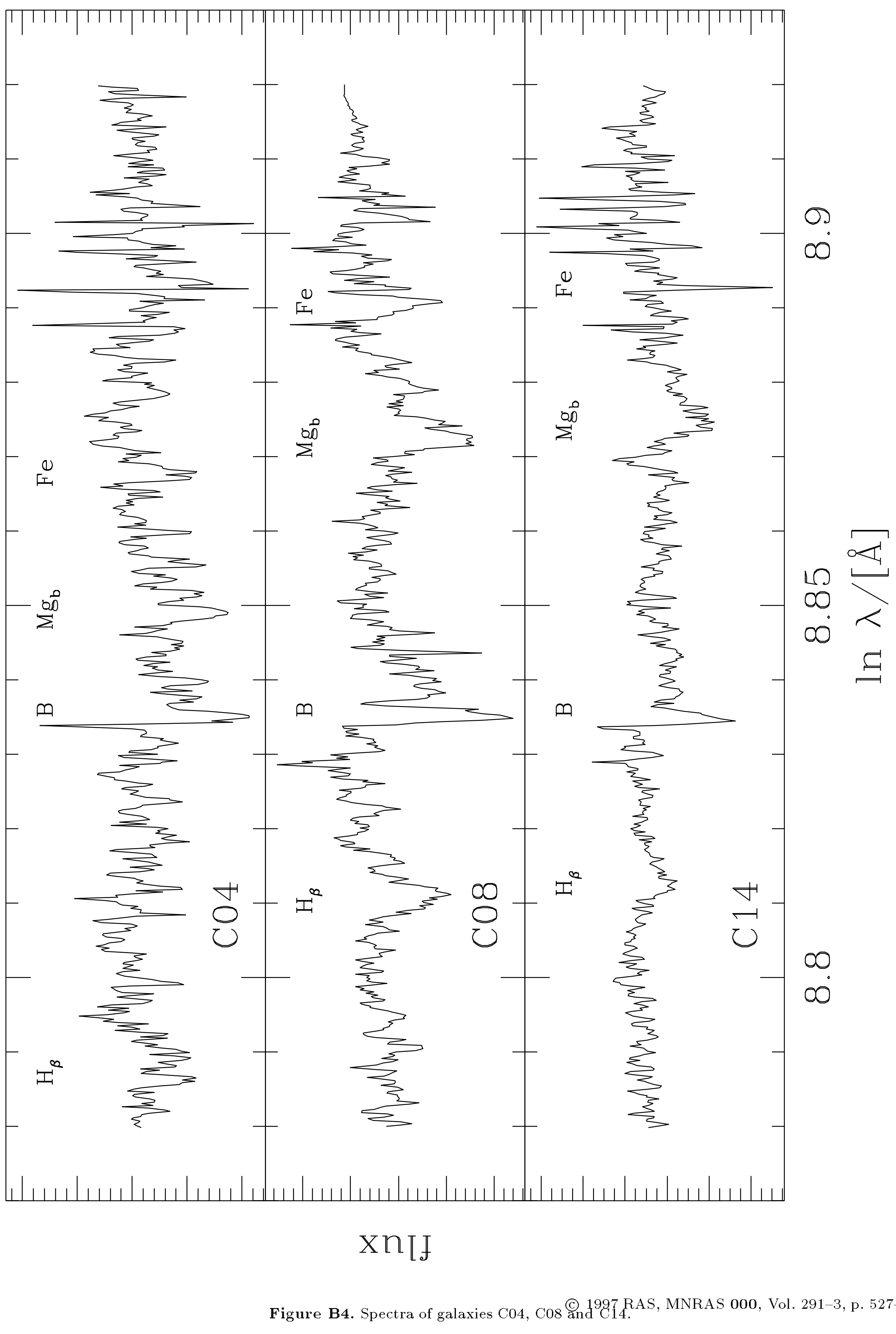

Figure B4. Spectra of galaxies C04, C08 and C14.

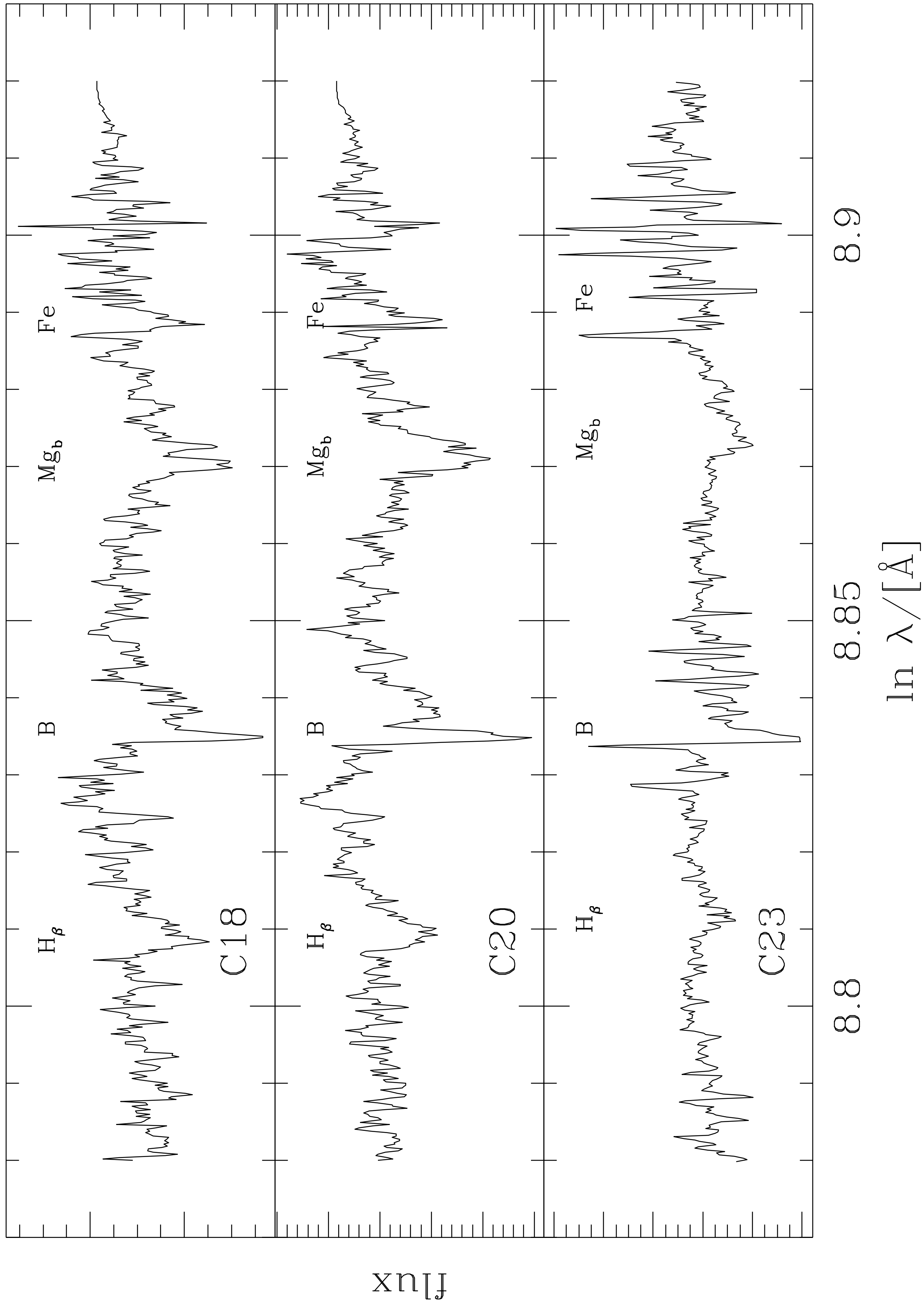

Figure B5. Spectra of galaxies C18, C20 and C23.

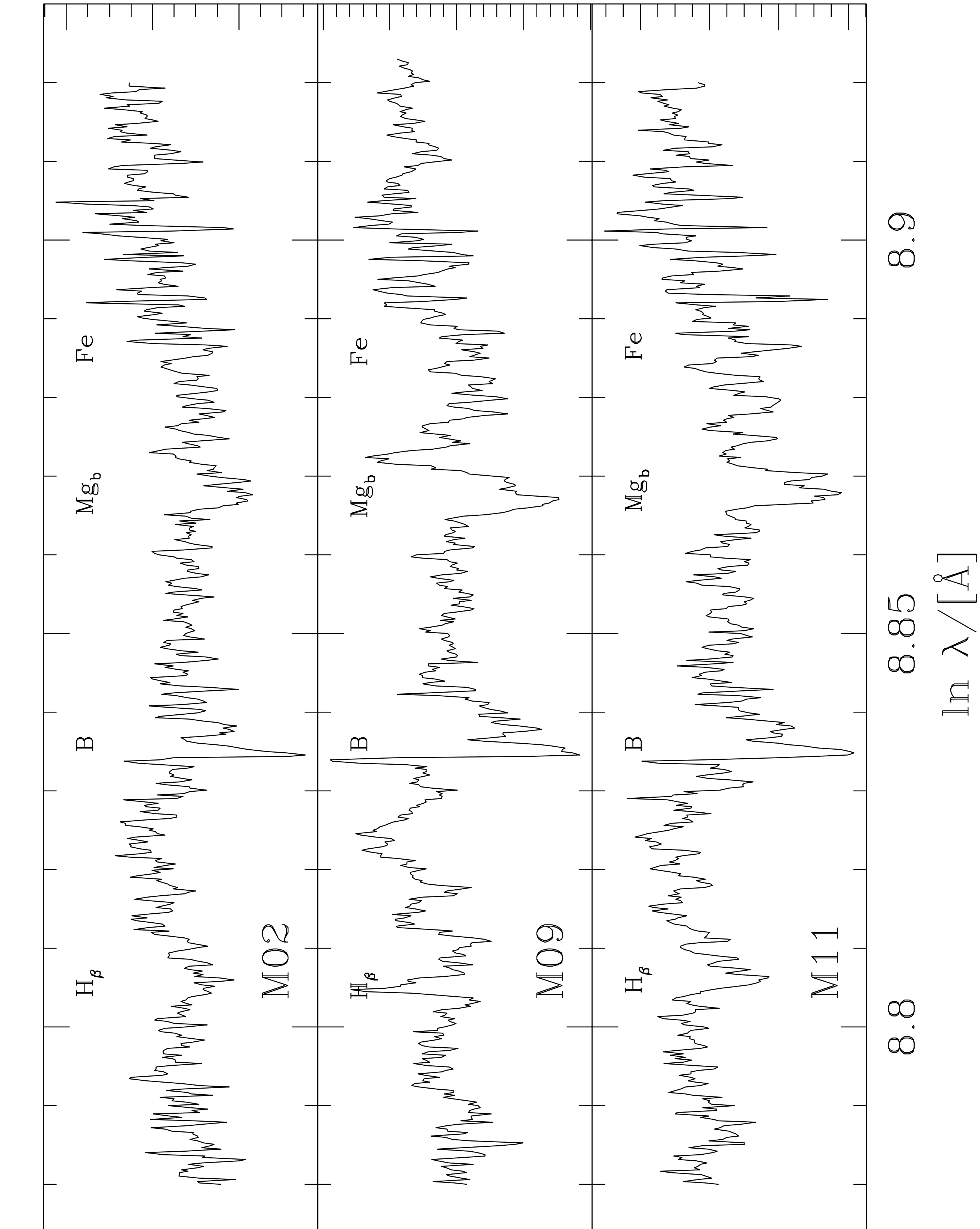

Figure B6. Spectra of galaxies M02, M09 and M11.

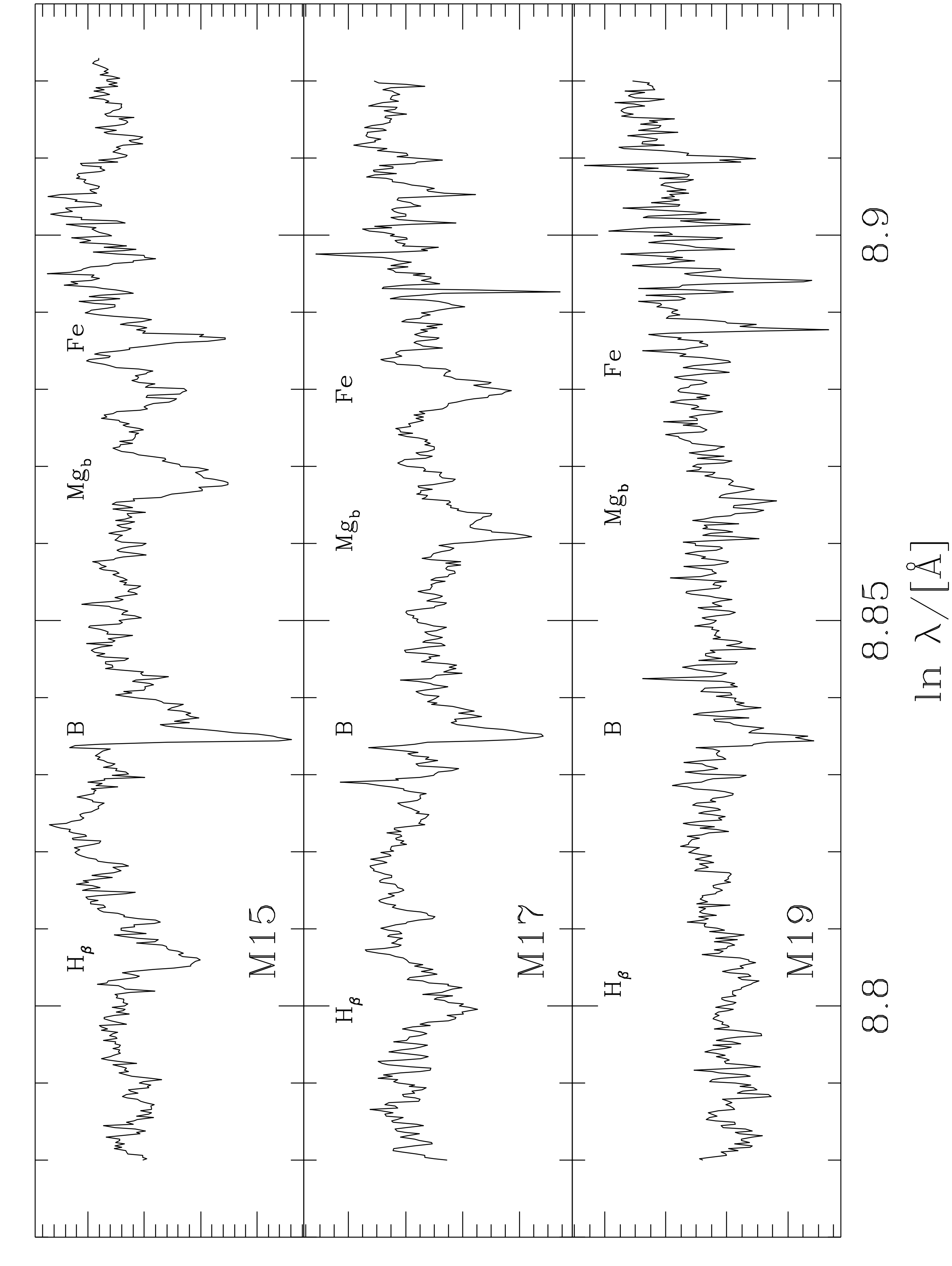

Figure B7. Spectra of galaxies M15, M17 and M19.